

University of Nevada, Reno

**Comparative Evaluation of Field and Laboratory-Produced Foamed Asphalt
Mixture from Reno, Nevada**

A thesis submitted in partial fulfillment of the
requirements for the degree of Master of Science in
Civil and Environmental Engineering

by

Christine Chia

Dr. Peter Sebaaly/Thesis Advisor

August, 2012

© by Christine Chia 2012

All Rights Reserved



University of Nevada, Reno
Statewide • Worldwide

THE GRADUATE SCHOOL

We recommend that the thesis
prepared under our supervision by

CHRISTINE CHIA

entitled

**Comparative Evaluation of Field and Laboratory-Produced Foamed Asphalt
Mixture from Reno, Nevada**

be accepted in partial fulfillment of the
requirements for the degree of

MASTER OF SCIENCE

Peter E. Sebaaly, Ph. D., Advisor

Elie Y. Hajj, Ph. D., Committee Member

Rajarantnam V. Siddharthan, Ph. D., Committee Member

Thomas Quint, Ph. D., Graduate School Representative

Marsha H. Read, Ph. D., Dean, Graduate School

August, 2012

ABSTRACT

This study evaluated the properties and performance of field-produced HMA and foamed WMA mixtures from the Bravo Ave project in Reno, Nevada in comparison to respective laboratory-produced mixtures utilizing the same materials and mix design. Each mixture contained 15% RAP and was produced with a polymer-modified PG64-28NV asphalt binder. The rheological properties were evaluated for virgin, RAP and extracted/recovered asphalt binders from field and plant-produced mixtures. The mixtures were evaluated for their resistance to moisture damage by means of measuring the dynamic modulus $|E^*|$ and the indirect tensile strength as a function of multiple freeze-thaw cycling. The resistance of the mixtures to permanent deformation was evaluated through the use of the repeated load triaxial (RLT) to measure the flow number (FN). The low-temperature cracking resistance of the mixtures was evaluated using the thermal stress restrained specimen test (TSRST).

From this study it was determined that the HMA had better resistance to moisture damage and permanent deformation than the foamed WMA mixtures. Between the HMA and foamed WMA mixtures, similar asphalt properties and resistance to thermal cracking were seen. The laboratory-produced mixtures did not exhibit similar behaviors as those seen with the field-produced mixtures. Also, reheating of the mixtures from an ambient temperature after mixing seems to only improve the resistance of the mixtures to moisture damage. The non-reheated mixtures had equal or better resistance to permanent deformation and thermal cracking than their reheated counterparts.

DEDICATION

I dedicate this work to my father, Nelson; my mother Lily; and to my amazing boyfriend Jake. Without the continuous and unrelenting support, patience, and love you three offer me every moment of every day, this whole journey would undeniably have been a near impossible accomplishment. You were the ones who offered not only your shoulders to lean on, and cry on occasionally, but you were also the ones who always helped me to see the silver lining through each grueling step of this whole process. Thank you so very much and I love you with all my heart.

ACKNOWLEDGMENTS

I would like to express my acknowledgement and appreciation to the University of Nevada, Reno, especially the Pavement/Materials Engineering program with the Civil and Environmental Engineering department for allowing me access to their facilities and providing me with the tools and means to accomplish my Master's work.

I would like to express my gratitude to Dr. Peter E. Sebaaly and Dr. Elie Y. Hajj for the support and guidance they offered me with throughout my course of study. They have trained me well and provided me with the tools and knowledge I need for a stable foundation to build and establish myself in the asphalt industry.

I would also like to express my sincerest appreciation and gratitude to my colleagues at school/work. Thank you so very much for helping me and establishing such great camaraderie, especially to Christine, Piratheepan, Kevin, Alvaro, Juan, Nate, Zahi, Marshall, Mena, Zia and last but definitely not least Nathan.

TABLE OF CONTENTS

Abstract	i
Dedication	ii
Acknowledgments.....	iii
Table of Contents	iv
List of Tables	vi
List of Figures	vii
Chapter 1: Introduction	1
1.1: Objective	2
1.2: Scope	2
Chapter 2: Background	4
2.1: WMA Technologies	6
2.2: Foamed WMA.....	7
2.3: Foaming Testing Equipment	8
2.4: Field Produced Mixtures in Comparison to Laboratory Produced Mixtures	11
Chapter 3: Field Project and Experimental Plan.....	14
3.1: Project Description.....	14
3.2: Experimental Program	15
3.3: Materials and Mix Design	17
3.4: Verification of Field Mixture Properties	17
Chapter 4: Description of Laboratory Tests.....	19
4.1: Properties of Asphalt Binders	19
4.2: Resistance to Moisture Damage.....	22
4.2.1: Dynamic Modulus	23
4.2.2: Indirect Tensile Strength	28
4.3: Resistance to Permanent Deformation	30
4.4: Resistance to Thermal Cracking	33
Chapter 5: Test Results and Analysis	36
5.1: Asphalt Binder Properties	36
5.2: Moisture Damage Resistance	36
5.2.1: Dynamic Modulus	36
5.2.2: Indirect Tensile Strength	38
5.3: Permanent Deformation Resistance	39
5.4: Thermal Cracking Resistance	40

Chapter 6: Findings and Recommendations	42
6.1: Findings	42
6.2: Recommendations	43
Chapter 7: Field Performance	44
References	45
Tables	49
Figures.....	55

LIST OF TABLES

Table 1 Compliance of the Polymer Modified PG64-28 NV Asphalt Binder Used on....	49
Table 2 Test Matrix for Mechanical Properties Evaluation.....	50
Table 3 Aggregate Gradation by Percent Passing and Bin Percentages Used.....	50
Table 4 Mix Design Summary and Specifications.	51
Table 5 Quality Assurance Testing Conducted by Wood Rogers on Bravo Avenue Field HMA and WMA Mixtures.....	52
Table 6 Asphalt Binder Content of Field Mixtures from Plant Production.....	53
Table 7 Superpave PG Grades of Various Asphalt Binders.	53
Table 8 Dynamic Modulus Values and Ratios of Field Mixtures at 10 Hz and 70°F.....	53
Table 9 Dynamic Modulus Values and Ratios of Laboratory Mixtures at 10 Hz and 70°F.	54
Table 10 Statistical Evaluation of Dynamic Modulus Results.	54

LIST OF FIGURES

Figure 1 Double Barrel Green® WMA System.....	55
Figure 2 Ultrafoam GX™ (Green Machine) WMA System.	55
Figure 3 Double Barrel Green® Manifold.....	56
Figure 4 Double Barrel Green® Nozzle Schematic.....	56
Figure 5 Maxam AQUABlack™ WMA System Unit Installed on a Drum Mix Plant. ...	57
Figure 6 AquaFoam Metering Skid.	57
Figure 7 AquaFoam Foaming Unit Installed in Asphalt Line.	58
Figure 8 Eco-Foam II Static Incline Vortex Mixer.....	58
Figure 9 Terex® WMA System.....	59
Figure 10 Tri-Mix Warm Mix Injection System.....	59
Figure 11 Pumping Skid for the Tri-Mix Warm Mix Injection System.	60
Figure 12 The Foamer and Disposable High Temperature Polymer Bag Manufactured by Pavement Technology, Inc.....	60
Figure 13 Location Map of Bravo Ave Field Project.	61
Figure 14 Study Experimental Program.	61
Figure 15 Cumulative Permanent Axial Strain with Respect to Number of Cycles.....	62
Figure 16 Typical Permanent Strain vs Loading Cycle Fitted with the Francken Model.	62
Figure 17 Coring of TSRST Samples.	63
Figure 18 Prepared TSRST Sample in Testing Chamber.	63
Figure 19 Superpave PG True Temperatures of Various Asphalt Mixtures.....	64
Figure 20 $ E^* $ of Field Mixtures at 70°F as a Function of F-T Cycles.....	65
Figure 21 $ E^* $ of Laboratory Mixtures at 70°F as a Function of F-T Cycles.	65

Figure 22 Dynamic Modulus and $ E^* $ Ratios of All Field and Laboratory-Produced Mixtures.	66
Figure 23 $ E^* $ Comparison of Mixtures Produced in the Field and the Laboratory.	67
Figure 24 $ E^* $ Ratio Comparison of Mixtures Produced in the Field and the Laboratory.	67
Figure 25 Tensile Strength of all Field-Produced Mixtures.	68
Figure 26 Tensile Strength of all Laboratory-Produced Mixtures.	68
Figure 27 Tensile Strength and Tensile Strength Ratio of All Evaluated Field and Laboratory-Produced Mixtures.	69
Figure 28 ITS Comparison of Mixtures Produced in the Field and the Laboratory.	70
Figure 29 ITS Comparison of Mixtures Produced in the Field and the Laboratory (Dry).	70
Figure 30 ITS Comparison of Mixtures Produced in the Field and the Laboratory (Wet).	71
Figure 31 TSR Comparison of Mixtures Produced in the Field and the Laboratory.	71
Figure 32 Flow Numbers at 58°C with 80 psi Deviator Stress and 30 psi Confining	72
Figure 33 Fracture Stresses and Temperatures of FMLC Mixtures. (Numbers represent mean values and whiskers represent mean \pm 95% confidence interval).	73
Figure 34 Photo for HMA and WMA Pavements on Bravo Avenue (May 18, 2011).	73
Figure 35 Photo for WMA and HMA Pavements on Bravo Avenue (July 17, 2012).	74
Figure 36 Maximum Rutting Depth of 1/16 Inches Measured (July 17, 2012).	74

CHAPTER 1: INTRODUCTION

Hot mix asphalt (HMA) has conventionally been extensively used for paving applications; however, there is a growing interest and trend in the use of warm mix asphalt (WMA) due to rising energy costs and more stringent environmental regulations. WMA mixtures allow for production, lay-down and compaction to occur at lower temperatures (30 to 100°F) in comparison to their HMA counterpart. WMA technologies that are currently popularly used include foaming (water-based) processes, wax-based additives, emulsion-based products, and surfactants. Regardless of whichever technology is used to produce a WMA mixture, the reduction in temperature is anticipated to have significant benefits such as reduced energy consumption, reduced plant emissions, better workability, and better compaction during construction, ability to incorporate higher percentages of RAP, and the capability for further hauling or seasonally later applications.

The predominate basis associated with any WMA technology revolves around the concept of lower the mixing and compaction temperatures of the produced mixture by manipulating the viscosity-temperature relationship of the asphalt binder. The reduced temperatures during mixing and compaction reduces the amount of short term aging to the asphalt binder which may allow for mixtures that are more durable and flexible and thus more resistant to cracking. The reduced temperatures associated with WMA also allows for the additional option of using WMA mixtures for cold weather applications whereas HMA is not a feasible option.

Regardless of all the promising benefits and advantages that WMA has to offer, the mixtures produced must still perform well in field applications as would be expected

from the traditional HMA mixtures. The produced WMA mixtures should still possess acceptable mechanical properties including high resistance to moisture damage, permanent deformation and thermal cracking as well as adaptable to the increasingly popular use of recycled asphalt pavement (RAP) in the mixtures.

1.1: Objective

The objective of this study was to evaluate the properties and performance of field-produced HMA and WMA mixtures from the Bravo Ave project in Reno, Nevada in comparison to respective laboratory-produced mixtures utilizing the same materials and mix design. The rheological properties were evaluated for virgin, RAP and extracted/recovered asphalt binders from field and plant-produced mixtures. The mixtures were evaluated for their resistance to moisture damage by means of measuring the dynamic modulus $|E^*|$ and the indirect tensile strength as a function of multiple freeze-thaw cycling. The resistance of the mixtures to permanent deformation was evaluated through the use of the repeated load triaxial (RLT) to measure the flow number (FN). The low-temperature cracking resistance of the mixtures was evaluated using the thermal stress restrained specimen test (TSRST).

1.2: Scope

This study evaluated the properties of field and laboratory-produced HMA and WMA mixtures from the Bravo Avenue field project in Reno, Nevada. Two types of pavement sections were paved on Bravo Avenue: an HMA control section and a section consisting of foamed WMA. Both the HMA and WMA mixtures incorporated 15% RAP and were designed using the Marshall Mix Design method for dense graded mixtures in accordance to specifications required by the Regional Transportation Commission (RTC)

and Granite Construction, Inc. For the evaluation of field-produced mixtures, loose plant-produced mixture was sampled at the plant at the time of discharge into tightly sealed buckets and brought back to the laboratory at the University of Nevada, Reno for evaluation. RAP, virgin aggregate and asphalt binder were also obtained and brought back to the laboratory for the production and evaluation of laboratory-produced mixtures. The approximate haul time between the production plant and the field project site were similarly 20 to 30 minutes as that from the production plant to the laboratory.

CHAPTER 2: BACKGROUND

For pavement applications in America, 94% of roads are surfaced with asphalt (1). The type of asphalt mixture traditionally used has been hot mix asphalt (HMA) mixtures; however, there is a growing interest and trend toward the use of warm mix asphalt (WMA) mixtures. Within the asphalt pavement industry, there is great need and desire to develop asphalt paving methods that adapts to increasing energy and material costs as well as toward more stringent environmental regulations. So far the asphalt pavement industry has done well to accommodate these changes and has even been implementing several government-mandated technologies as well as continuing to seek innovations further promoting a cleaner planet and better working conditions for workers (2).

WMA in general refers to a group of technologies which allow a reduction in the temperatures (30 to 100°F) at which asphalt mixtures are produced and placed (3). There are a lot of benefits and advantages associated with WMA that make it significant. WMA technologies tend to provide better and complete aggregate coating even at the lower temperatures and act as compaction aids. The reduction in production temperatures not only provides numerous benefits related to sustainable development and improved working conditions, but it also has a wide range of potential benefits that includes and is not limited to the following (2):

- Paving benefits
 - Reduced compaction effort,
 - Ability to pave in cool ambient temperatures without sacrificing quality,

- Ability to haul asphalt pavement mixtures further distances for longer durations and still have the necessary workability to place and compact the mixture,
- Ability to incorporate higher percentages of recycled asphalt pavement (RAP), while producing the mixture at reasonable temperatures, and facilitating placement and compaction,
- Minimizing or eliminating bumps and crack when placing asphalt over crack sealant,
- Reduced fuel consumption
- Reduced plant emissions, including greenhouse gas emissions
- Better working conditions

There have been concerns that the reduced production temperatures may impair the hardening of the asphalt binder, or hinder the evaporation of moisture from aggregates, leading to an increased occurrence of rutting and an increase incidence of moisture damage in asphalt concrete pavements, respectively. There may also be further asphalt mixture interactions that affect other performance properties of an asphalt concrete pavement depending on the warm-mix technology.

Several research studies have consistently reported that WMA shows greater potentials for moisture damage and rutting than conventional HMA when evaluated using conventional laboratory procedure (4, 5, 6, 7). However, reported field data showed generally good performance, particularly with respect to moisture damage and rutting with premature failures often being associated with construction issues or plant malfunctions (4, 5). At the time of construction, the WMA mixtures showed lower tensile

strength than HMA; however, after two years in service, the tensile strength of the WMA was similar to the HMA mixtures (5, 6, 8).

2.1: WMA Technologies

The various WMA technologies may be classified into different categories based on certain factors, such as the degree of temperature reduction; however, WMA technologies are commonly classified as those that are foamed (water-based) processes, wax-based additives, emulsion-based products, or as surfactants.

WMA processes that use organic additives or waxes show a decrease in viscosity above the melting point of the wax. The type of organic additive or wax used should be carefully selected so that the melting point of the additive is higher than the expected in-service temperatures in order to reduce the risk of permanent deformation. The low-temperature properties of the asphalt binder may also be affected by the type of organic additive or wax used; however, this effect may be partially mitigated in the WMA through the use of reduced production temperatures. WMA processes that use chemical additives or surfactants primarily rely on a various different mechanisms to improve aggregate coating at the lower temperatures used as well as provide a lubricity effect to reduce compaction efforts. Water-based processes introduce small amounts of water to hot asphalt, either via a foaming nozzle, damp aggregate or mineral filler that slowly releases moisture internally. The premise of water-based WMA relies in the fact that the water causes a volume expansion of the asphalt binder, which decreases the viscosity and improves aggregate coating as well as compaction. (2).

2.2: Foamed WMA

Among the various WMA technologies available nowadays, an increased use of the water-based technologies is being observed in the United States, particularly with the Double Barrel® Green and the Ultrafoam GX™ foaming systems, respectively shown in Figures 1 and 2. Both of the systems utilize proprietary foaming nozzles to inject a percentage of water (typically 1-2% by weight of binder) into the asphalt binder flow line. The introduction of water causes an immediate volume increase of the asphalt binder, or the foaming effect, as the liquid surface area increases. The water also temporarily lowers the asphalt binder viscosity while improving uniform aggregate coating and mixture workability at the lower WMA temperatures.

The Double Barrel Green® WMA system uses a multi-nozzle foaming device to microscopically foam the asphalt. As for the Ultrafoam GX™ system, also known as the Green Machine, the unit uses only the energy supplied by the pump or head supplying the asphalt binder to achieve the foaming process. This eliminates the need for a powered mixing device, like Advera® WMA and Aspha-min® would require in order to properly blend the synthetic zeolites containing 20 percent water of crystallization with the asphalt binder, allowing the asphalt binder to be introduced at various flow rates, temperatures, and pressures, resulting in more consistent asphalt foaming at different production rates.

The Accu-Shear™ assembly allows water, WMA chemical additives, other liquid additives, or any liquid combination thereof, to be simultaneously injected into the asphalt line. A variable speed colloidal mill is used to blend the water or other additives. Similar to an emulsion process, the shearing process of the colloidal mill mechanically blends the liquids. The rate of shear may be adjusted by the variable speed drive to

dynamically foam the asphalt, which the manufacturer believes increases the life of the foam.

Another foamed WMA process is conducted by the LEA (Low Emission Asphalt) process, otherwise known as Low Energy Asphalt outside the United States. In this process, the coarse aggregate is heated to greater temperatures (approximately 302°F or 150°C) and then is mixed with the total binder required for the mixture at the normal binder temperature that is appropriate for the particular grade used. A coating and adhesion additive by weight of binder is added to the binder just prior to mixing. Once the coarse aggregate is coated, it is mixed with the unheated and wet (ideally containing 3 to 4% water) fine aggregate or blend of fine aggregate and RAP. The moisture turns to steam and causes the asphalt on the coarse aggregate to foam, which then encapsulates the fine aggregate.

2.3: Foaming Testing Equipment

Focusing specifically on testing equipment that produces the foaming effect, there are the previously mentioned Double Barrel Green® WMA system and Ultrafoam GX™; however, there are various others including the AQUABlack™ WMA System, AquaFoam foaming system, Eco-Foam II, Terex® WMA System, Tri-Mix Injection System, and The Foamer. Each of these foaming devices mentioned above are briefly introduced and described below.

The Double Barrel Green® WMA system, seen in Figure 1, is mostly composed of a manifold, seen in Figure 3, with a system of valves, mixing chambers, and nozzles. The multi-nozzle foaming device, nozzle schematic seen in Figure 4, microscopically foams the asphalt by injecting water into the mixing chamber. The water being supplied

to the system is regulated by a positive displacement pump and meter whose speed varies based on the speed of the asphalt pump. One pound of water is added per ton of mix, and a small percentage of this water is encapsulated in the binder as steam. The binder volume is increased by this steam.

The Ultrafoam GX™ System, sometimes referred to as the Green Machine and seen in Figure 2, uses only the energy supplied by the pump or head supplying the asphalt binder to achieve the foaming effect. The system uses approximately 1.25 to 2 percent water by weight of total asphalt binder. The water is added by injection into the center of the asphalt flow line. A centrally located spring-loaded water valve is opened when water pressure is applied. Located externally to the nozzle, a diaphragm plate allows the asphalt binder to flow at varying rates while maintaining a constant fluid pressure. The ratio of asphalt binder and water, if well-maintained, is supposed to create smaller steam bubbles for more consistent asphalt foaming.

The AQUABlack™ WMA System, seen in Figure 5 and developed by Maxam Equipment Inc., uses a patented, stainless steel foaming gun in conjunction with a center convergence nozzle to produce the foaming effect. Maxam Equipment Inc. utilizes the self-developed MicroBubble™ foaming technology to produce microbubbles. The MicroBubble foaming technology uses water pressures up to 1,000 pounds psi (6895 kPa) to create greater expansion of the foam, or the microbubbles. The AQUABlack™ WMA System utilizes the precedence of high water pressure for more bubbles to increase workability.

The AquaFoam foaming system mounts two fan nozzles 180 degrees to one another, and the nozzles are mounted perpendicular to the asphalt stream. Asphalt is

prevented from back flowing into the water system by a one-way check valve. A variable-frequency-drive pump delivers the required water to the nozzles. The controls, pump, and a 65 gallon tank are mounted on a skid pump, which can be seen in Figure 6. The water flow is metered by a high-resolution pulse counter, and the water tank includes a water-level switch. The system is attached to the blending system of a plant in a manner similar to liquid anti-stripping agent addition, as seen in Figure 7.

Eco-Foam II, also known as the AESCO/MADSEN Static Inline Vortex Mixer and shown in Figure 8, uses the principle of shear zone turbulence to enhance the mixing and foaming process. This process also uses vortex shedding, which happens when a specific fluid produces oscillations after it passes an obstruction. The alternating low-pressure zones created by these oscillations are used to aid in the mixing process. The foaming process is initiated with the delivery of liquid asphalt binder to the Vortex mixer and is forced through the mixer restriction, which creates a high-speed flow. Water or other liquids (i.e. additive, liquid anti-stripping agent) is injected downstream from the mixer tabs and into the low-speed, reversed flow region at a rate of 1 to 2 percent of the liquid asphalt flow rate. The difference in addition rates accelerates the mixing of the asphalt binder and additive/water by increasing the contact area between the high and low-speed fluids. Once the asphalt and additive/water combines and becomes a single fluid, it encounters obstructions and creates the oscillations that enhance the foaming effect. The foamed asphalt can then enter the mixer once the fluid leaves the Vortex mixer.

The Terex® WMA System, illustrated in Figure 9, uses a patented, single expansion chamber to provide an asphalt binder and water mixture at any desired

production rate. The system simply requires a jacketed asphalt binder line and water feed pipes to be supplied by the contractor. The foam is produced by the Terex WMA System outside the drying drum then is immediately injected into the mixing drum for even aggregate coating.

The Tri-Mix Warm Mix Injection System is a 24 inch long foaming unit that is hot-oil jacketed and uses two opposed high pressure injection nozzles followed by a downstream static mixer to foam the asphalt or water-based chemical additive. The Tri-Mix Foaming System, displayed in Figure 10, uses a variable-frequency drive pump and the controls are mounted on a separate pumping skid, seen in Figure 11. For cold weather operations, there is a heating package available for the skid.

The Foamer manufactured by Pavement Technology, Inc. is a foaming device designed for laboratory use which allows ease of movement in tandem with a laboratory mixer. The mobile unit, seen in Figure 12, has adjustable dispensing height and accommodates up to 14 pounds (6.35 Kilograms) of asphalt binder. The reservoir is lined with a special high temperature disposable polymer bag, also seen in Figure 12, which can be discarded upon completion of test, allows for easy cleanup, minimum residual asphalt, and allows batches to be sequentially run with no clean up.

2.4: Field Produced Mixtures in Comparison to Laboratory Produced Mixtures

While most studies revolve around the different and various WMA technologies, the testing equipment to accommodate and achieve them, and the feasibly successful implementation of their applications as a paving material, the studies that compare plant-produced asphalt mixtures from the field to laboratory-produced asphalt mixtures are limited in comparison. From the available studies that do compare field and laboratory

WMA asphalt mixtures, the resulting trends vary from one another. In a study by Iskender et al. (9), one of the primary issues they encountered revolved around duplicating the composition of a field mixture in the laboratory, which further exasperates the issue of when trying to produce a specimen in the laboratory that truly represents the mixture as it exists in the field (10). Iskender et al. determined from the results of their study that their laboratory mixtures exhibited better performance than the field mixtures. However, in a study conducted by Tran et al. (11) at the National Center for Asphalt Technology (NCAT), they concluded from their results that their field WMA mixtures performed equal or better than their laboratory-produced mixtures. The fact that there is no consistent laboratory conditioning procedure for preparing WMA specimens for performance tests is the entire premise for the study being conducted by Yin et al. (12). A standard protocol is essential for accurate evaluation of mix performance. The AASHTO Standard R 30 *Standard Practice for Mixture Conditioning of Hot Mix Asphalt* establishes a procedure for preparing HMA specimens for performance testing. The practice of conditioning laboratory samples is required to accurately simulate the binder absorption and aging that occurs during construction, and it is generally achieved by short-term oven aging the loose mixture at a certain temperature for a certain period after mixing and prior to compaction. Some laboratory conditioning protocols of WMA technology have been proposed to achieve similar laboratory performances between WMA and the control HMA or similar performance between mixtures prepared in the laboratory and field specimens (9, 11, 12). The most common trend indicated by these studies is that an increase in conditioning time and/or temperature reduces the difference in performance between HMA and WMA. Without a consistent laboratory conditioning

procedure for WMA technology being established already, there is also the issue that different WMA technologies may require different conditioning protocols due to differences in components (i.e. surfactants, organic or chemical additives) (2, 12).

CHAPTER 3: FIELD PROJECT AND EXPERIMENTAL PLAN

This comparative evaluation of field and laboratory-produced foamed asphalt mixture revolves around the field project of Bravo Avenue located in Reno, Nevada. Information provided in this chapter applies to project description, materials, mix design and the experimental plan.

3.1: Project Description

In August 2010, a foamed warm mix asphalt (WMA) road section, as well as a control section of hot mix asphalt (HMA), were placed along Bravo Avenue in Reno, Nevada by the Regional Transportation Commission (RTC) and Granite Construction, Inc. Both field mixtures, which were produced at the Granite Construction plant in Lockwood, Nevada, were made with a polymer-modified PG64-28NV asphalt binder, 15% recycled asphalt pavement (RAP) and 1.5% hydrated lime by the dry weight of virgin aggregate added on damp aggregate. Table 1 shows the test results of the PG64-28NV asphalt binder for compliance with Nevada specifications. The WMA mixture was produced using the Ultrafoam® process at an average water injection rate of 1.25% by weight of binder. At the field project location, the mixtures were placed into a total thickness of 6 inches with two 3 inch lifts.

Referring to Figure 13, Bravo Avenue is located just south of the Reno-Stead Airport. The field project spans from the intersection of Mount Limbo Street to Ramsey Way for an approximate 1.5 miles. Bravo Avenue is a two-lane road where the HMA was paved in the eastbound lane and the WMA paved in the westbound lane. The operational speed of Bravo Avenue is slow at 20 mph; however, the roadway experiences a lot of military vehicle traffic.

The temperature of the WMA, when leaving the plant, ranged between 265 and 275°F. An average lay-down temperature of 250 and 255°F was determined and consequently used in the WMA laboratory evaluations. The HMA mixture had a lay-down temperature of 305°F. Upon construction, no issues related to the use of foamed WMA with RAP were observed and the required in-place densities were met.

3.2: Experimental Program

The plant-produced mixtures that were placed in the field were sampled at the plant at the time of discharge into tightly-sealed buckets and brought back to the Pavement/Materials laboratory at the University of Nevada, Reno (UNR) for evaluation. Additionally, virgin aggregates, RAP and asphalt binder were sampled prior to production for laboratory reproduction of the field plant-produced mixtures. The reproduced laboratory WMA samples were produced using The Foamer device from Pavement Technology, Inc. (PTI).

The field mixtures were compacted at the UNR laboratory for mechanical properties after a maximum of 4 hours short-term oven aging in sealed containers at the corresponding lay-down temperatures (i.e., 305°F for HMA and 255°F for WMA). The approximate haul time between the plant and the UNR laboratory was similarly 20 to 30 minutes as that between the plant and the project paving site. Additionally, the mechanical properties were evaluated for samples reheated from ambient temperatures to 275°F in the oven, for 4 hours, followed by 2 hours at the corresponding lay-down temperature before compaction. The reheated laboratory-produced samples were also placed in sealed buckets and split into appropriate sample proportions as the field-

produced mixtures. The following nomenclatures were used throughout this study for the various evaluated mixtures:

- FMLC_HMA_NoReheat and FMLC_WMA_NoReheat: HMA and WMA field mixture, respectively, produced by the plant and compacted after a maximum of 4 hours short-term oven aging in sealed containers at the corresponding lay-down temperatures.
- FMLC_HMA_Reheat and FMLC_WMA_Reheat: HMA and WMA field mixture, respectively, produced by the plant and compacted post reheating from ambient temperatures for 4 hours at 275°F, followed by 2 hours at their corresponding lay-down temperatures.
- LMLC_HMA_NoReheat and LMLC_WMA_NoReheat: HMA and WMA laboratory-produced mixture, respectively, both produced and compacted at the UNR laboratory. Compaction occurred after similar 4 hour maximum short-term oven aging as the FMLC mixtures at the corresponding lay-down temperatures.
- LMLC_HMA_Reheat and LMLC_WMA_Reheat: HMA and WMA laboratory-produced mixture, respectively, both produced and compacted at the UNR laboratory. Compaction occurred after similar reheating as the FMLC mixtures from ambient temperatures for 4 hours at 275°F, followed by 2 hours at their corresponding lay-down temperatures.
- LMLC_HW_NoReheat and LMLC_HW_Reheat: HMA produced and compacted at WMA temperatures in the UNR laboratory upon similar respective short-term oven aging or reheating procedures as the HMA and WMA mixtures.

Figure 14 shows the experimental program for this comparative evaluation. It consisted of the following two major aspects:

- Rheological properties of virgin, RAP and extracted/recovered asphalt binders from various field and laboratory-produced mixtures.
- Mechanical properties of field and laboratory-produced mixtures according to the test matrix as shown in Table 2. The resistance of the mixtures to moisture damage, permanent deformation and thermal cracking were evaluated respectively by means of: dynamic modulus testing ($|E^*|$), indirect tensile strength (IDT) and tensile strength ratio (TSR) at multiple freeze-thaw cycles; repeated load triaxial (RLT); and by thermal stress restrained specimens testing (TSRST).

3.3: Materials and Mix Design

The WMA and HMA mixtures from the Bravo Ave field project were designed by Granite Construction Inc. using the Marshall Mix Design method for HMA (13). The asphalt binder was produced by Paramount Petroleum in Fernley, Nevada and consisted of a modified PG64-28NV binder. Aggregates treated with 1.5% hydrated lime to mitigate moisture damage susceptibility, from Granite's aggregate pit in Lockwood, Nevada, was used as the aggregate source for the entire comparative evaluation between field and laboratory-produced mixtures. Table 3 provides the aggregate gradation by percent passing and the bin percentages used. Table 4 summarizes the primary mix design data along with the corresponding specifications.

3.4: Verification of Field Mixture Properties

Quality assurance (QA) testing performed by Wood Rogers as a third party was conducted on numerous core samples obtained from each of the various Stations sampled

from along Bravo Avenue. The results from the QA testing can be seen in Table 5. The in-place densities, measured as a percent of maximum theoretical density, were well within the typically acceptable range of 91 to 98% (14). The asphalt content of each of the obtained samples was determined by the ignition oven method (15), and they were found to be within the specifications of the project. Each of the aggregate samples retained from the ignition oven method were also sieved for gradation and determined to be within specifications. No issues in obtaining the appropriate air-void percentages were observed either. The stability and flow of the samples also met specifications for the Marshall Mix Design used for the Bravo Avenue field project.

Some verification testing was also conducted by those from the UNR laboratory. A sieve analysis performed on extracted aggregates, according to AASHTO T308 and T30 specifications, from the plant mixtures sampled during production revealed that the aggregate gradation was well controlled with respect to the job mix formula (JMF). The asphalt binder contents of the asphalt mixtures from Bravo Avenue were determined during production using the ignition oven method, according to AASHTO T308 specifications, and averages are shown in Table 6 along with the 95% confidence interval. Both mixtures, HMA and WMA from the field, met the corresponding asphalt binder content JMF.

CHAPTER 4: DESCRIPTION OF LABORATORY TESTS

The objective of this study was to evaluate the properties and performance of field-produced HMA and WMA mixtures from the Bravo Ave project in Reno, Nevada in comparison to respective laboratory-produced mixtures utilizing the same materials and mix design. The rheological properties were evaluated for virgin, RAP and extracted/recovered asphalt binders from field and plant-produced mixtures. The mixtures were evaluated for their resistance to moisture damage by means of measuring the dynamic modulus ($|E^*|$), the indirect tensile strength (IDT) and the indirect tensile strength ratio (TSR) as functions of multiple freeze-thaw cycling. The resistance of the mixtures to permanent deformation was evaluated through the use of the repeated load triaxial (RLT) to measure the flow number (FN). The low-temperature cracking resistance of the mixtures was evaluated using the thermal stress restrained specimen test (TSRST).

4.1: Properties of Asphalt Binders

Prior to the development of current binder specifications, such as the Superpave specifications, the tests conducted and used to determine binder grades were empirical and could not meaningfully characterize the relationship between the tests and performance of the binders: the tests did not provide information for the entire range of typical pavement temperatures (low, medium, and high). Binders that were determined to have the same grading, based on the previous and strictly empirical test methods, could display entirely different temperature and performance characteristics. Therefore, in 1987 the Strategic Highway Research Program began developing new tests for measuring the physical properties of asphalt binders, which resulted in a new set of test equipment and

procedures that were adopted by American Association of State Highway and Transportation Officials (AASHTO) and American Society for Testing and Materials (ASTM) (16). The Superpave binder tests, which are conducted at temperatures that are encountered by in-service pavements, can measure and directly relate the physical properties of asphalt binders to field performance based on engineering principles.

The Superpave binder tests are conducted at conditions that represent the three critical stages experienced by binder during its life. Tests conducted on original binder simulate the first stage where transport, storage and handling occur. The binder is then aged in a rolling thin film oven (RTFO), exposing thin films of binder to heat and air, which simulates the mix production and construction stage of the binder. In the third stage, the binder is subjected to heat and pressure for an extensive period of time in a pressure aging vessel (PAV) in order to simulate the in-service aging conditions experienced by the binder as part of the asphalt pavement layer over a long period of time.

The viscous and elastic behavior of asphalt binders at high and intermediate service pavement temperatures may be characterized and determined through the respective $G^*/\sin\delta$ and $G^*\sin\delta$ parameters as in accordance to the AASHTO Standard T 315 *Determining the Rheological Properties of Asphalt Binder Using the Dynamic Shear Rheometer (DSR)* standard. For testing with the DSR, 25 mm or 8 mm diameter samples of binder for respective high or intermediate temperature testing are sandwiched between two parallel plates, a fixed bottom plate and an oscillating top plate, and sheared at a frequency of 10 radians per second, or 1.59 Hz, to simulate truck loading at 40-50 mph. The complex shear modulus (G^*) value indicates the total resistance of the binder to

deformation when repeatedly sheared and consists of two components: the elastic modulus G' and the viscous modulus G'' . The phase angle (δ) indicates the time lag between the applied shear stress and the corresponding shear strain, or rather indicates the relative amounts of recoverable and non-recoverable deformation. A binder with a phase angle equal to 0° is a purely elastic material, with no viscous component, since shear stresses and strains occur simultaneously. When the phase angle is equal to 90° , the binder is a purely viscous material due to a long delay between and applied shear stress and the corresponding shear strain. Asphalt binders behave like viscous fluids at high temperatures with no capacity for recovering or rebounding. Asphalt binders behave like elastic solids at very low temperatures which rebound from deformation completely. Under normal pavement temperatures the characteristics of both a viscous fluid and elastic solid are in play; therefore, the binder is described as viscoelastic.

The low service temperature characteristics may be determined through the creep stiffness (S) and creep rate (m -value) parameters as in accordance to AASHTO Standard T 313 *Determining the Flexural Creep Stiffness of Asphalt Binder Using the Bending Beam Rheometer (BBR)* standard. The BBR rather than the DSR is used to evaluate the binder properties at low pavement temperature since asphalt binders are too still to reliably measure properties at low temperatures when using the parallel plate geometry of the DSR. Regardless, with the combined use of the DSR and BBR, the stiffness behavior of asphalt binders over a wide range of temperatures may be determined. The BBR test is performed on binders that have been short-term aged through the RTFO and that have also been long-term aged through the PAV. The low temperatures at which the BBR test is performed correlates with the lowest service temperature of the pavement, which can be

used to estimate failure or strength properties, but mostly to measure how much a binder deflects or creeps under a constant load at a constant temperature when the asphalt binder acts more like an elastic solid. As indicated by the name, the BBR test method utilizes the concept of a simply supported beam to calculate the stiffness of an asphalt binder beam sample under a creep load. The center deflection of the beam is measured as a constant load is applied and then used to calculate the creep stiffness and creep rate. The creep load simulates thermal stresses that gradually build up in a pavement as temperatures decrease while the resistance of the asphalt binder to creep loading is the creep stiffness. The change in asphalt stiffness with time during loading is determined by the m-value.

For the Bravo Ave project, the virgin, RAP and recovered blended binders from the various plant and laboratory-produced loose mixtures were graded by the Superpave Performance Grading (PG) binder system (19). All recovered binders were extracted using a centrifuge (19) and recovered using a rotary evaporator (20) using a solution of 85% Toluene and 15% Ethanol by volume. The critical temperatures, or temperatures at which a binder meets the appropriate specified Superpave criteria, were determined and therefore used to determine the PG grades of the various binders.

4.2: Resistance to Moisture Damage

When asphalt pavements are exposed to moisture, there is a major concern for moisture susceptibility and damage spawning from either adhesion failure or cohesion failure or even a combination thereof (21). The pavement distress from the weakening of the bond between the aggregates and asphalt binder due to the intrusion of moisture reduces the mixture strength or the strength of the pavement itself (22).

The resistance of the various Bravo Ave mixtures to moisture damage was evaluated using the measurement of the dynamic modulus ($|E^*|$), indirect tensile strength (IDT) and indirect tensile strength ratio (TSR) as functions of multiple freeze-thaw (F-T) cycling. The process of F-T cycling was conducted as defined by AASHTO T-283 but at multiple stages. A total of three samples from each mixture were evaluated at each of the unconditioned (0 F-T) and moisture-conditioned stages after 1 and 6 F-T cycles for both test procedures.

4.2.1: Dynamic Modulus

For effective comparison between field and laboratory-produced mixtures, samples prepared for moisture damage performance testing by means of $|E^*|$ evaluation, were compacted at air-void levels of 6.5 ± 0.5 %, which were obtained with the field-produced mixtures that were compacted right away. Sample preparation for $|E^*|$ testing was conducted as follows:

- Compact the 6” diameter cylindrical specimens to a height of 7” in the Superpave Gyrotory Compactor (SGC) and core them into 4” diameter samples with a 6” height,
- Measure the unconditioned $|E^*|$ master curve (i.e., 0 F-T cycles),
- Subject the samples, to be F-T conditioned, to 75 ± 5 % saturation,
- Subject the saturated samples to multiple F-T cycles, wherein one full F-T cycle consists of freezing at 0°F (-18°C) for a minimum of 16 hours followed by 24 ± 1 hours thawing in a water bath at 140°F (60°C) and concluding with 2 ± 0.5 hours in a water bath at 77°F (25°C),
 - Subject each sample to the required number of F-T cycles,

- Conduct $|E^*|$ testing after the respective number of F-T cycles.

Per the AASHTO PP 61-10 standard, the results from the dynamic modulus test were used to develop the dynamic modulus ($|E^*|$) master curve of the mixtures. The $|E^*|$ property of the various mixtures is evaluated under various combinations of loading frequencies and temperatures in order to evaluate the structural response of the asphalt pavement under various combinations of traffic loads, speed, and environmental conditions. A sinusoidal (haversine) axial compressive stress is applied to a specimen at a given temperature and loading frequency during testing. The frequencies used during testing consisted of 25, 10, 5, 0.5, 0.1 Hz and the temperatures that the testing was conducted at consisted of 40, 70, 100 and 130°F (4.4, 21.1, 37.8 and 54°C, respectively). The dynamic modulus is then calculated from the measured applied stress and resulting recoverable axial strain response of the specimen. Due to the viscoelastic behavior of an asphalt mixture (i.e. interchangeability of the effect of loading rate and temperature), the master curve can be used to identify the appropriate $|E^*|$ for any combination of pavement temperature and traffic speed (23). The general quality of the asphalt mixtures may be inferred from the $|E^*|$ property; therefore, the relationship between $|E^*|$ and the number of F-T cycles provides an excellent indication of the moisture resistance of the asphalt mixtures.

A mathematical expression for $|E^*|$ is shown in Equation 4.1.

$$|E^*| = \frac{\sigma}{\varepsilon} = \frac{\sigma_0 e^{i\omega t}}{\varepsilon_0 e^{i(\omega t - \phi)}} = \frac{\sigma_0 \sin \omega t}{\varepsilon_0 \sin(\omega t - \phi)} = E' + iE'' \quad (4.1)$$

Where;

$|E^*|$ = complex dynamic modulus

E' = storage modulus

E'' = loss modulus

σ_0 = peak (amplitude) stress

ε_0 = peak (amplitude) strain

ϕ = phase lag or angle expressed in degrees

ω = angular velocity in radians per second

t = time, seconds

$$i = \sqrt{-1}$$

The E value is generally referred to as the storage (elastic) modulus component of the complex modulus, while E'' is referred to as the loss (viscous) modulus. The loss tangent ($\tan \phi$) is the ratio of the energy lost to the energy stored in a cyclic deformation as shown in Equation 4.2.

$$\tan \phi = \frac{E''}{E'} \quad (4.2)$$

In uniaxial compression in mathematical terms, the absolute value of the complex dynamic modulus is defined as the maximum (peak) dynamic stress (σ_0) divided by the amplitude of the recoverable axial strain (ε_0).

$$|E^*| = \frac{\sigma_0}{\varepsilon_0} \quad (4.3)$$

Equation 4.4 displays the sigmoidal function representing the $|E^*|$ master curves, and Equation 4.5 provides the general form of the shift factors, which defines the relationship between actual time of loading and reduced time. The relationship between the actual time of loading and reduced time can be rewritten as Equation 4.6.

$$\log(|E^*|) = \delta + \frac{\alpha}{1 + e^{\beta + \gamma \log(t_r)}} \quad (4.4)$$

$$t_r = \frac{t}{a(T)} \quad (4.5)$$

$$\log(t_r) = \log(t) - \log[a(T)] \quad (4.6)$$

Where;

t_r = time of loading at the reference temperature

α, δ = fitting parameters; (for a given set of data, δ represents the minimum value of $|E^*|$, and $\alpha + \delta$ represents the maximum value of $|E^*|$)

$\beta + \gamma$ = parameters describing the shape of the sigmoidal function

$a(T)$ = shift factor as a function of temperature

T = temperature of interest

t = time of loading at a given temperature of interest.

The AASHTO MEPDG dictates that at a given temperature of interest, $a(T)$ can be expressed in terms of asphalt binder viscosity and time of loading, which can be seen in Equation 4.7. The parameter c is one of the values returned by the numerical optimization. The shift factor depends only on the binder viscosity for the age and temperature of interest, and the RTFO-aged viscosity at the reference temperature.

$$\log(a(T)) = -c(\log(\eta) - \log(\eta_{T_R})) \quad (4.7)$$

Where;

T = temperature of interest

$a(T)$ = shift factor as a function of temperatures

η = viscosity of the asphalt binder at temperature of interest, cP

η_{T_R} = viscosity of the asphalt binder at reference temperature and RTFO aging, cP.

With a reference temperature of 70°F (21°C), the master curve is constructed using the principle of time-temperature superposition (*t-TS*) and then the data is shifted at various temperatures with respect to time until the curves merge into a single smooth function. The *t-TS* principle is only valid in the linear viscoelastic region and is only applicable to thermo-rheologically simple materials, which includes most bituminous materials. The curve shape does not change for bituminous materials when a change of temperature shifts the modulus vs. time/frequency curve along time/frequency axis (24). The relationship between asphalt binder viscosity and temperature must be established prior to shifting the mixture data, which when using Equation 4.8, may be accomplished by first converting the binder stiffness data at each temperature to viscosity. The binder complex modulus and phase angle data are determined over a range of temperatures for a loading of 1.59 Hz (10 rad/sec) using the DSR. The parameters of the A-VTS equation (Equation 4.9) are found by linear regression of Equation 4.9 after a log-log transformation to the viscosity data and log transformation of the temperature data.

$$\eta = \frac{G^*}{10} \left(\frac{1}{\sin \delta} \right)^{4.8628} \quad (4.8)$$

$$\log \log \eta = A + VTS \log T_R \quad (4.9)$$

Where;

η = viscosity, cP

G^* = binder complex shear modulus, Pa

δ = binder phase angle, °

A = regression intercept

VTS = regression slope of viscosity temperature susceptibility

T_R = temperature in Rankine at which the viscosity was determined.

The binder viscosity may be calculated at any temperature using the regression parameters from Equation 4.9; however, this equation is not applicable at low temperatures and high rates of loading where the binder viscosity exceeds 2.7×10^{10} Poises. If the binder viscosity data is not available, the reduced time in Equation 4.4, may be computed using shift factors as a function of temperature with Equation 4.10.

$$\log|E^*| = \delta + \frac{\alpha}{1 + e^{\beta + \gamma(\log t - \log[a(T)])}} \quad (4.10)$$

4.2.2: Indirect Tensile Strength

The moisture susceptibility of the various Bravo Ave mixtures were also evaluated using the unconditioned and moisture-conditioned indirect tensile strengths (ITS) as well as the indirect tensile strength ratio (TSR) after multiple F-T cycles as proscribed by AASHTO T283. This procedure indicates the effect of water intrusion through saturation and the consequential results by means of accelerated water conditioning with the F-T cycling of the compacted asphalt mixture samples.

For effective comparison between field and laboratory-produced mixtures, samples prepared for moisture damage performance testing by means of IDT and TSR| evaluation, were compacted at air-void levels of 5.5 ± 0.5 % for HMA and 7.0 ± 0.5 % for WMA, which were obtained with the field-produced mixtures that were compacted right away. These air-void levels do not match the design air-voids for the field project; however, the respective air-voids for HMA and WMA match between FMLC and LMLC samples. HMA samples prepared and compacted at WMA temperatures were compacted

at air-void levels consistent for WMA samples. At least 15 samples were prepared for each mixture and divided into three subsets of three samples each: unconditioned subset (i.e. 0F-T), moisture-conditioned subset to 1 F-T, and moisture conditioned subset to 3 F-T. Sample preparation for IDT and TSR testing was conducted as follows:

- Compact the 4” diameter cylindrical specimens to a height of 2.5” in the Superpave Gyrotory Compactor (SGC).
- Measure the ITS for the unconditioned subset (i.e., 0 F-T cycles) at 77°F (25°C). The unconditioned subsets were acclimated to the required temperature by submerging the samples, wrapped and contained in leak-proof plastic bags, into a water bath set to the required temperature. Submergence of samples in the water bath were for 2 ± 0.5 hours.
- Subject each of the three samples from both the moisture-conditioned subsets to $75 \pm 5\%$ vacuum-saturation. A vacuum partial pressure of 10 to 26 in. HG was applied for a short period of time (5 to 10 minutes).
- Subject the saturated samples to multiple F-T cycles, wherein one full F-T cycle consists of freezing at 0°F (-18°C) for a minimum of 16 hours followed by 24 ± 1 hours thawing in a water bath at 140°F (60°C) and concluding with 2 ± 0.5 hours in a water bath at 77°F (25°C),
 - Subject each sample to the required number of F-T cycles,
- Measure the ITS after the respective number of F-T cycles.
- Calculate the TSR after the respective number of F-T cycles.

4.3: Resistance to Permanent Deformation

Permanent deformation, in regards to asphalt pavements, are permanent changes in the shape of the pavement or pavement layers which can manifest through distorting distresses as rutting and shoving (25). Mostly found in urbanized areas and especially at intersections, shoving occurs where heavy vehicles move slowly or stop frequently. Shoving is caused by the shear flow in the mixture or inter-layer/lift slippage. On the other hand, rutting is caused by the progressive movement of materials under repeated loads, either in the asphalt pavement layers or the underlying base, and it can occur either through consolidation or through lateral plastic flow. Consolidation is the further compaction of asphalt pavement by traffic after construction. In comparison to that from plastic flow, the amount of rutting from consolidation is generally relatively insignificant with other factors remaining constant. As a result from traffic loads, rutting occurs in the wheel paths of the pavement.

The resistance of the various Bravo Ave asphalt mixtures to rutting was evaluated through the use of the repeated load triaxial (RLT) test to measure the flow number (FN). Cylindrical samples were subjected to a static confining pressure and a repeated haversine deviator stress that is applied for an appropriate pulse (loading) time and a rest (unloading) period. The axial deformation of each of the tested samples is measured and the cumulative permanent axial strain is calculated and plotted with respect to the number of loading cycles. The plot is defined by three stages: primary, secondary and tertiary, with the FN being the point at which the tertiary flow begins. The three zones are described below and shown in Figure 15:

- Primary stage: Permanent strain increases rapidly producing a high initial level of rutting with a decreasing rate of plastic deformations. This is mainly due to a rearrangement of the structure of the mixture with an eventual concentration of stresses in the contact surface between the loading plate and sample due to small irregularities (26), predominantly associated with volumetric change. Researchers have shown that densification is unlikely with pavements well compacted during construction and its contribution, if any, is only at the first working stage of asphalt pavement (27).
- Secondary stage: Permanent strain rate maintains a constant value that is also associated with volumetric changes; however, as shear deformations increase at an increasing rate, the tertiary creep zone is reached. Lower rates of deformation (slope of accumulated strain vs. load repetitions) during the secondary stage of the uniaxial repeated loading test suggest a more stable mixture after initial densification has been achieved, and the structure of the mixture has finished its relocation due to initial traffic compaction (26).
- Tertiary stage: High level of permanent axial strain predominantly associated with plastic or shear deformations under no volume change conditions. Basically, this stage is reached when the specimen is beginning to deform significantly and individual aggregates composing the skeleton of the mixture are moving past each other. The point at which the tertiary flow starts is called the flow number. Meaning, the FN is defined as the number of load cycles corresponding to the minimum rate of change of permanent axial strain.

Through the use of the predictive equations developed by Hajj et al. (28), the appropriate RLT test parameters of confining and deviator stresses were determined for a 6-inch thick asphalt layer.

Provided that the operational speed for the Bravo Ave field project is 20 mph, the determined RLT test parameters consisted of a respective 0.05 and 0.09 second pulse and rest period. The confining and deviator stresses used, dependent upon operational speed, asphalt layer temperature and stiffness, were 30 and 80 psi. The RLT tests were conducted at 58°C. The temperature was determined as the effective pavement temperature 2 inches below the pavement surface as indicated by the LTPPBind software for the given location.

The most commonly used methods to determine the FN from the cumulated permanent deformation versus loading cycle number data included the Three-Stage Method, the Stepwise Increase Approach and the Francken Model Method. The FNs for the Bravo Ave field project were determined using the Francken Model Method.

The Francken method was developed based on triaxial repeated load tests under various temperatures and stress levels and is a combination of a power law function with an added exponential function (29). The model is obtained through a complex regression mathematical model as shown in Equation 4.1.

$$\varepsilon_p(N) = AN^B + C(e^{DN} - 1) \quad (4.1)$$

Where;

ε_p = plastic/permanent axial strain,

N = number of loading cycles, and

A, B, C, D = regression constants.

Once the regression constants are obtained, the first derivative of Equation 4.1 with respect to N is obtained, as shown in Equation 4.2, to generate the strain rate.

$$\frac{\delta \varepsilon_p(N)}{\delta N} = (A \cdot B \cdot N^{(B-1)}) + (C \cdot D \cdot e^{DN}) \quad (4.2)$$

Finally, the second derivative of the Francken model is then computed at each cycle to obtain the rate of change of the slope of permanent strain as presented in Equation 4.3. The cycle number at which the tertiary stage is reached, or FN, is then computed at the point where the rate of change of slope changes sign (goes from negative to positive). This point indicates the inflection point in the permanent strain versus number of cycle's curve where the tertiary stage begins.

$$\frac{\delta^2 \varepsilon_p(N)}{\delta N^2} = A \cdot B \cdot (B - 1)N^{(B-2)} + (C \cdot D^2 \cdot e^{DN}) \quad (4.3)$$

The regression constant C in the Francken model indicates whether tertiary flow has occurred or not. The Francken model also provides a good representation of all three stages of deformation (i.e. flow) including the tertiary stage (30). Figure 16 shows the Francken model fitted to typical repeated load test data. Through a large series of FN tests conducted on field mixtures by Dongre et al (31), the use of the Francken model was further validated as a means for determining FN and found to produce fits with low statistical error.

4.4: Resistance to Thermal Cracking

The low-temperature cracking resistance of the various Bravo Ave mixtures was evaluated using the thermal stress restrained specimen test (TSRST) according the AASHTO TP10-93 standard to determine the fracture stress and fracture temperature. The test chills a 2.25-inch diameter specimen with a 5.5-inch height at a rate of

10°C/hour while restraining it from contracting: the ends are epoxy-glued to fixed plates. The fracture temperature represents the temperature at which the asphalt mixture will crack due to thermal stresses, while the fracture stress represents the magnitude of stress caused by the thermal contraction of the mixture. As the temperature decreases, and with the ends restrained, the internally generated stresses of the specimen will eventually exceed its tensile strength, which is when the fracture occurs. However, the fracture stress controls the spacing of thermal cracks once they occur. It is believed that a greater fracture stress in the TSRST indicates a longer spacing between the transverse cracks of a pavement in the field. Figure XX shows the general setup of the TSRST as well as a typical thermal stress versus temperature relationship for asphalt mixtures.

The TSRST test was only performed for the field-produced Bravo mixtures. The TSRST specimens began as cylindrical 6-inch diameter samples compacted to a height of 7-inches to an air-voids level of 6.5 ± 0.5 %, which were obtained with the field-produced mixtures that were compacted right away. All TSRST samples were long-term aged following the Superpave recommendation for long-term aging of HMA mixtures which consists of subjecting the compacted samples to 185°F for 5 days in a forced draft laboratory oven. The long-term aging of the samples simulates the fact that low-temperature cracking is a long-term pavement distress. After being subjected to long-term aging, the 6" x 7" cylindrical samples were cored and cut twice from the side, as seen in Figure 17, in order to obtain two cylindrical samples that are 2.25-inches in diameter and 5.5 inches in height. These smaller cylindrical samples are then glued to plates for restraint and conditioned to 5°C in a freezer for a minimum of 6 hours to bring them to

the starting test temperature. Figure 18 displays a prepared and glued TSRST in the testing chamber ready for testing.

CHAPTER 5: TEST RESULTS AND ANALYSIS

5.1: Asphalt Binder Properties

The critical temperatures for each of the evaluated binders, or temperatures at which the binder meets the appropriate specified Superpave criteria for high, medium and low temperatures, are shown in Figure 19. These temperatures indicate the true binder grades of the binder, and the PG grades for the various evaluated binders are indicated in Table 7. The high temperature grade for each of the evaluated binders met or exceeded the target grade of 64°C for the project; however, not all of the extracted and recovered binders met the low temperature target grade of -28°C. The binders that did not meet the low temperature target grade consisted of those extracted and recovered from reheated field-produced mixtures as well as all of the laboratory-mixtures. On the other hand, each of the critical temperatures for these mixtures was between the critical temperatures determined for the virgin and RAP binders. This indicates that a hundred percent, complete blending of the virgin and Rap binder occurred through the extraction and recovery process. The virgin binder was the least stiff, with the RAP binder being the stiffest, and each of the extracted and recovered binders had PG Grades in between.

5.2: Moisture Damage Resistance

5.2.1: Dynamic Modulus

The $|E^*|$ values at 70°F (21°C) and 10 Hz as functions of F-T cycling are respectively shown in Figures 20 and 21 for all field and laboratory-produced asphalt mixtures. The $|E^*|$ ratios for all of the field and laboratory-produced mixtures are respectively displayed in Tables 8 and 9. Figure 22 displays the $|E^*|$ and $|E^*|$ ratio of all field and laboratory-produced mixtures. The $|E^*|$ of field-produced mixtures in

comparison to their respective laboratory-produced counterparts are shown in Figure 23, while Figure 24 shows the $|E^*|$ ratios for the field versus laboratory comparison.

The $|E^*|$ dramatically decreases between the unconditioned state (0 F-T) and the first moisture conditioned state (1 F-T) for both field and laboratory-produced mixtures. For the field-produced mixtures, the decrease in $|E^*|$ from the first moisture conditioned state (1 F-T) to the second moisture conditioned state (6 F-T) was slight in comparison to the decrease seen with the laboratory mixtures. The reheated mixtures also had only a slight decrease between the two moisture conditioned states in comparison to their non-reheated counterparts. A summary of the statistical analysis conducted for the dynamic modulus results can be seen in Table 10. When evaluating the differences between the field and laboratory-produced mixtures, the mixture type (i.e. HMA vs. WMA) was found to not be statistically significant, neither was the relationship between the mixtures that were reheated or not, meaning that the field and laboratory-produced mixtures exhibited similar trends with their mixtures between the two different heating states; however, there was a highly significant influence seen from the F-T cycling on the $|E^*|$ values. As for the mixtures that were strictly field-produced, the mixture type, type of heating and the F-T cycling were each found to be statistically highly significant. On the other hand, the opposite was discovered within the laboratory-produced mixtures: the mixture type and the heating state were not found to be statistically significant and the F-T cycling was found to be highly statistically significant. Last but not least, there were no statistical differences between the HMA and WMA mixtures aside from the influence of F-T cycling on the mixtures. Overall, the WMA mixtures exhibited similar moisture resistance in comparison to HMA, and the reheated mixtures seem more resistant to

moisture damage than their non-reheated counterparts. Aside from the amount of decrease in $|E^*|$ with each F-T cycle, the field mixtures were statistically similar to the laboratory-produced mixtures.

5.2.2: Indirect Tensile Strength

The tensile strength at 77°F (25°C) as functions of F-T cycling for all field and laboratory-produced mixtures are respectively shown in Figures 25 and 26. Figure 27 shows the tensile strength ratio of all field and laboratory produced mixtures. The tensile strength of field-produced mixtures in comparison to their laboratory-produced mixture counterparts are shown in Figures 28 through 30. Figure 28 shows the tensile strength comparison for all conditioned states (i.e. 0, 1, 6 F-T) for the field and laboratory-produced mixtures, while Figures 29 and 30 respectively show only the tensile strengths at the unconditioned state (i.e. 0 F-T) and the moisture conditioned states (i.e. 1 & 6 F-T). Figure 31 shows the tensile strength ratios of field-produced mixtures in comparison to their laboratory-produced mixture counterparts.

The minimum value of 80% for the TSR was not met by all mixtures. Within the field-produced mixtures, each of the mixtures had TSR values greater than 80% after 1 F-T cycle, and only the reheated HMA mixture did not have a TSR value greater than 80% after 6 F-T cycles. As for the laboratory-produced mixtures, none of the mixtures had TSR values greater than 80% after being subjected to 6 F-T cycles; however, only the reheated HMA mixture did not meet the minimum after 1 F-T cycle.

For both field and laboratory-produced mixtures, the HMA mixtures, reheated or not, had greater tensile strength values than either the WMA or the HMA at WMA mixtures. The reheated mixtures exhibited similar tensile strength values as their non-

reheated counterparts. Also, within the laboratory-produced mixtures, the WMA and HMA at WMA mixtures had similar tensile strength values to each other. Between the each state of level of conditioning, the field mixtures had a slight decrease in tensile strength while the laboratory mixtures had a greater decrease in tensile strength. Initially, at the unconditioned state, each of the mixtures, whether they were field or laboratory-produced, had statistically similar values with overlapping confidence intervals; however, the moisture conditioned samples reduced at different rates from 1 F-T cycle to 6 F-T cycles between the field and laboratory-produced mixtures. This suggests that the laboratory-produced mixtures are more susceptible to moisture damage than the field-produced mixtures.

5.3: Permanent Deformation Resistance

The resistance to permanent deformation for each of the evaluated field and laboratory-produced mixtures were evaluated by the RLT test. The samples used for testing were not subjected to long-term aging since permanent deformation is predominately a short-term pavement distress. The analysis of the results was conducted with the use of the Francken Method to determine the FN for each mixture, which is shown in Figure 32. Only the non-reheated component from the laboratory-produced mixtures is included in the analysis to date. For the duration of this thesis, there was an unexpected failure with the testing equipment, which has delayed the results for the reheated laboratory-produced mixtures; however, these mixtures shall be evaluated upon reestablishment of the testing equipment.

As seen in Figure 32, the non-reheated field-produced HMA mixture has the highest FN with the reheated laboratory-produced WMA mixture having the lowest FN.

Each of the HMA mixtures have greater FN values than the WMA mixtures, regardless of whether they were reheated or not. This suggests that the foamed WMA mixtures have less resistance to permanent deformation in comparison to HMA. Even the HMA at WMA mixture seems to have greater resistance to permanent deformation than the WMA mixture within the laboratory-produced mixtures. In regards to field-produced mixtures in comparison to the laboratory-produced mixtures, each of the field-produced mixtures exhibit better resistance to permanent deformation than their respective laboratory-produced counterpart. This may suggest that the field-mixtures experience greater aging than the laboratory mixtures, leading to stiffer mixtures in general, and thus exhibits that greater resistance trend.

As for the non-reheated laboratory-produced WMA mixture, no FN can be determined by analyzing the RLT results with the Francken Method. The transition from the secondary to the tertiary stage was too subtle for the Francken Method to cipher: rather than the tertiary stage displaying an exponential behavior, it was linear. Therefore, it is under review for the analysis method to be reconsidered and perhaps use another method, such as the Three-Step Method, to reanalyze the results.

5.4: Thermal Cracking Resistance

Figure 33 shows the determined fracture stresses and fracture temperature of the various mixtures evaluated with the TSRST. The HMA and WMA mixtures have statistically similar fracture stresses and fracture temperatures with the overlapping confidence intervals. The fracturing stresses occurred at fracture temperatures lower than the determined low temperature grade of the extracted and recovered binders for those respective mixtures. This suggests that a hundred percent complete blending of the RAP

and virgin binder did not occur during mixing for these mixtures. Regardless, the results suggest that thermal cracking would occur at temperatures lower than the target low temperature grade of the binder used for the field project.

The low temperature cracking resistance was only evaluated for the field-produced samples to date. For the duration of this thesis, there was an unexpected failure with the testing equipment, which has delayed the testing for additional mixtures; however, these mixtures shall be evaluated upon reestablishment of the testing equipment.

CHAPTER 6: FINDINGS AND RECOMMENDATIONS

6.1: Findings

- Both the high and low temperature grades for the extracted and recovered binders were bumped up from the target grades.
- The PG grades of the extracted and recovered binders from the asphalt mixtures were between those for the virgin binder and the binder extracted and recovered from the RAP, thus indicating that a hundred percent, complete mixing had occurred.
- From the dynamic modulus testing, the mixture types were overall statistically similar in their resistance to moisture damage; however, the laboratory mixtures were less resistant to moisture damage than the field mixtures.
- The HMA mixtures had greater tensile strength than the WMA mixtures; however, the tensile strength ratios were similar and sometimes better for the WMA mixtures than the HMA mixtures.
- Similar to the dynamic modulus testing, the laboratory-produced mixtures were more susceptible to moisture damage than the field-produced mixtures when evaluating in terms of tensile strength ratios.
- From E^* and RLT testing, lab mixtures seem stiffer than field mixtures.
- The HMA mixtures had better rutting resistance than WMA mixtures.
- Field Mixtures had better rutting resistance than laboratory mixtures.
- Each of the field-produced mixtures, regardless of whether they were reheated or not, displayed similar resistance to thermal cracking with overlapping confidence intervals for both fracture stress and fracture temperature.

- The fracture temperatures determined for the field-produced mixtures occurred at lower temperatures than the low temperature grade determined from the analysis of binder properties. This indicates that a hundred percent, complete blending did not occur between the virgin and RAP binder.
- Overall, similar trends between field and laboratory-produced mixtures were not observed.
 - Dynamic modulus of the laboratory mixtures decreased more rapidly with each F-T cycle than the field mixtures.
 - Tensile strength and tensile strength ratio declined more rapidly with each F-T cycling for laboratory mixtures than field mixtures.

6.2: Recommendations

- In addition to the evaluation of mechanical properties between HMA and foamed WMA mixtures, the volumetric properties should also be evaluated.
- When an evaluation of volumetric properties is conducted, the impact of curing time on these volumetric properties should also be evaluated.
- A standard short-term oven aging procedure should be used for laboratory-produced mixtures to better replicate properties and performance of field-produced mixtures.
- The actual compaction effort required compacting the samples to N92 and N98 should also be evaluated through the use of devices that dynamically measure the forces present during compaction in order to further enhance the credibility of WMA requiring less compaction effort than HMA.
- 2D-imaging analysis should be conducted to evaluate aggregate coating by asphalt binder and aggregate orientation within the mixtures.

CHAPTER 7: FIELD PERFORMANCE

In May 2011, a field visual inspection was performed for the Bravo Ave project. Figures 34 show a photograph taken at the time of assessment. The inspection revealed no distresses in the HMA and WMA mixtures after 9 months of service. Overall, the pavement condition was excellent and uniformly the same along the total length of the project.

In July 2012, another field visual inspection was performed and pictures taken during this assessment are shown in Figures 35 and 36. The inspection still revealed no distresses in the HMA and WMA mixtures, even after 23 months of service. Aside from a maximum of 1/16 inch rutting measured, seen in Figure 35, the overall pavement condition was excellent and uniformly the same along the total length of the project.

REFERENCES

1. Asphalt Pavement Alliance. (-) "Asphalt Pavement: America Rides on Us". At: http://asphaltroads.org/documents/Asphalt_White_Paper_doc.pdf. Last Visit: July 28, 2012.
2. Prowell, B., G., Hurley, and B., Frank. "Warm-Mix Asphalt: Best Practices", National Asphalt Pavement Association (NAPA) Quality Improvement Publication 125, Second Edition, 2011.
3. Kazosi, A. "Properties of Warm Mix Asphalt from two field projects: Reno, NV and Manitoba, Canada", University of Nevada, Reno Masters of Science Thesis, Reno, Nevada, 2010.
4. Abbas, A. R. and A., Ali. "Mechanical Properties of Warm Mix Asphalt Prepared Using Foamed Asphalt Binders". Final Report FHWA/OH-2011/6, Federal Highway Administration, Springfield, Virginia, 2011.
5. Hurley, G., B., Prowell, and A., Kvasnak. "Ohio Field Trial of Warm Mix Asphalt Technologies: Construction Summary". NCAT Report 09-04, National Center for Asphalt Technology, Auburn, AL, 2009.
6. Hurley, G., B., Prowell, and A., Kvasnak. "Missouri Field Trial of Warm Mix Asphalt Technologies: Construction Summary". NCAT Report 10-02, National Center for Asphalt Technology, Auburn, AL, 2009.
7. Bonaquist, R. *Mix Design Practices for Warm Mix Asphalt*. NCHRP Report 691, Transportation Research Board of the National Academics, Washington, D.C., 2011.
8. Kvasnak, A., A., Taylor, J., Signore, and S. A. Bukhari. "Evaluation of Gencor Green Machine Ultrafoam GX". NCAT Report 10-03, National Center for Asphalt Technology, Auburn AL, 2010.
9. Iskender, E., A., Aksoy. "Field and Laboratory Performance Comparison for Asphalt Mixtures with Different Moisture Conditioning Systems", Construction and Building Materials, 27th Volume, 2012.
10. Goetz, W.H. "The Evaluation of Asphalt Concrete Mix Design". ASTM STP 1041; 1989.
11. Tran, N., A. J., Taylor. "Moisture Resistance of Sulfur-Modified Warm Mix". NCAT Report 11-07, National Center for Asphalt Technology, Auburn Al, 2011.

12. Yin, F., L., Garcia. "Laboratory Conditioning Protocols for Warm-Mix Asphalt", Association of Asphalt Paving Technologies (AAPT) Student Poster, Austin, TX, 2012.
13. Asphalt Institute. *Mix Design Methods for Asphalt Concrete and Other Hot Mix Types*, Manual Series Book MS-2, Sixth Edition, Lexington, KY, 1997.
14. Killingsworth, B.M. *Quality Characteristics for Use with Performance Related Specifications for Hot Mix Asphalt*. NCHRP Project 9-15 Research Results Digest 291, Washington, D.C.: Transportation Research Board, National Research Council, 2004.
15. American Society of Testing and Materials (ASTM) Designation D 6307, "Standard Test Method for Asphalt Content of Hot-Mix Asphalt by Ignition Method", 2009.
16. Asphalt Institute. *Performance Graded Asphalt Binder Specification and Testing*, Superpave Series Book SP-1. Lexington, KY, 1995.
17. Kvasnak, A., J., Moore, A., Taylor, and B. Prowell. "Preliminary Evaluation of Warm Mix Asphalt Field Demonstration: Franklin, Tennessee". NCAT Report 10-01, National Center for Asphalt Technology, Auburn, AL, 2010.
18. Wielinski, J., A., Hand, and D.M., Rausch. "Laboratory and Field Evaluations of Foamed Warm-Mix Asphalt Projects". In *Transportation Research Record: Journal of the Transportation Research Board*, No. 2126, Transportation Research Board of the National Academies, Washington, D.C., 2009, pp. 125-131.
19. American Association of State Highway and Transportation Officials (AASHTO). *Standard Specifications for Transportation Materials and Methods of Sampling and Testing*. 29th Edition, Washington, D.C., 2010.
20. American Society of Testing and Materials (ASTM) Designation D 5404, "Standard Practice for Recovery of Asphalt from Solution Using the Rotary Evaporator", 2003.
21. Hughes, C. S. and Maupin, G.W., Jr., "Factors that Influence Moisture Damage in Asphaltic Pavements", *Implication of Aggregates in the Design, Construction, and Performance of Flexible Pavements, ASTM STP 1016*, H.G Schreuders and C.R Marek, Eds, American Society for Testing and Materials, Philadelphia, 1989, pp 96-102.
22. Pavement Interactive. (-) "Moisture Susceptibility". At: <http://www.pavementinteractive.org/article/moisture-susceptibility/>. Last Visit: August 4, 2012.

23. National Cooperative Highway Research Program (NCHRP), “Guide for Mechanistic-Empirical Design of New and Rehabilitated Pavement Structures”, Transportation Research Board, National Research Council, February 2004.
24. Anderson, D. and Rowe, G., “Rheology of Asphalt Binders and Implications for Performance”, Webinar, November 10, 2009.
25. Roberts, F. L., Kandhal, P.S., Brown, E. R., Lee, D., and Kennedy, T. W., “Hot Mix Asphalt Materials, Mixture Design, and Construction”, Second Edition, National Asphalt Pavement Association Research and Education Foundation, 1996.
26. Archilla, A., Diaz, L., and Carpenter, S. “Proposed Method to Determine the Flow Number from Laboratory Axial Repeated Loading Tests in Bituminous Mixtures”, Transportation Research Board, TRB, Washington, D.C., 2007
27. Eisenmann, J. and Hilmer, A., “Influence of Wheel Load and Inflation Pressure on the Rutting Effect at Theoretical Investigations”. 6th International Conference on the Structural Design of Asphalt Pavements, University of Michigan, Ann Arbor, Michigan, 1987, pp. 392-403.
28. Hajj, E. Y., A., Ulloa, R. Siddharthan, and P.E., Sebaaly. “Estimation of Stress Conditions for the Flow Number Simple Performance Test”. In *Transportation Research Record: Journal of the Transportation Research Board*, No. 2181, Transportation Research Board of the National Academics, Washington, D.C. , 2010, pp. 67-78.
29. Francken, L. “Permanent Deformation Law of Bituminous Road Mixes in Repeated Load Triaxial Compression”, *Proceeding of Fourth International Conference on the Structural Design of Asphalt Pavements*, University of Michigan, Ann Arbor, MI, United States, (1977).
30. Biligiri, K. P., Kaloush, K. E., Mamlouk, M.S., and Witczak, M. W. “Rational Modeling of Tertiary Flow for Asphalt Mixtures”, *Transportation Research Records*, Vol. 2001, TRB, National Research Council, Washington, D.C. (2007).
31. Dongre, R., D’Angelo, J., Copeland, A. “Refinement of Flow Number as Determined by the Asphalt Mixture Performance Tester for Use in Routine QC/QA Practice”, Transportation Research Board, TRB, Washington, D.C. (2009).
32. Federal Highway Administration (FHWA). “LTPPBind Software”. Long-Term Pavement Performance program, Version 3.1.
33. Witczak, M. W. “Effective Temperature Analysis for Permanent Deformation of Asphaltic Mixtures”, A-001 MIDAS Study. September 1992.

34. Pavement Technology, Inc. (-) "The Foamer". At:
<http://www.pavementtechnology.com/products/TheFoamer.asp>. Last Visit: July 30, 2012.

TABLES

Table 1 Compliance of the Polymer Modified PG64-28 NV Asphalt Binder Used on Bravo Avenue to Nevada Specifications.

TESTS	NEV#	AASHTO #	SPEC	RESULT
Test on Original Asphalt:				
Viscosity, 135°C (275°F), Pa.s		T316	3.00 max	0.75
DSR, G*/sinδ, 64°C @ 10 rad/s, kPa		T315	1.00 min	1.67
Flash Point, C.O.C., °F	T716	T48	450 min	550+
Ductility, 4°C (39.2°F), 5cm/min, cm	T746	T51	50 min	60
Toughness, inch-lbs	T745		110 min	162
Tenacity, inch-lbs	T745		75 min	148
Specific Gravity, T1/T7°F		T228	—	1.0162
Specific Gravity, 60/60°F		T228	—	1.0222
API Gravity, 60°		T228	—	6.9
Sieve Test, Particles Retained	T730		0	0
Test on Residue from Rolling Thin Film Oven:				
DSR, G*/sinδ, 64°C @ 10 rad/s, kPa		T315	2.20 min	3.25
Ductility, 4°C (39.2°F), 5cm/min, cm	T746	T51	25 min	30
Loss on Heating, wt. %		T240	1.0 max	0.340
Test on Residue from Pressure Aging Vessel @ 100°C				
DSR, G*/sinδ, 22°C @ 10 rad/s, kPa		T315	5000 max	1905
Creep Stiffness, S, -18°C @ 60s, Mpa		T313	300 max	122
Creep Stiffness, m-value, -18°C @60s, Mpa		T313	0.300 min	0.320

Table 2 Test Matrix for Mechanical Properties Evaluation.

Mechanical Property	Mixture ID									
	FMLC_HMA_NoReheat	FMLC_WMA_NoReheat	FMLC_HMA_Reheat	FMLC_WMA_Reheat	LMLC_HMA_NoReheat	LMLC_WMA_NoReheat	LMLC_HW_NoReheat	LMLC_HMA_Reheat	LMLC_WMA_Reheat	LMLC_HW_Reheat
Resistance to Moisture Damage - E* vs. Freeze-Thaw (F-T): 3 samples at 0, 1 & 6 F-T - IDT & TSR vs. F-T: 3 samples at 0, 1, & 6 F-T	X	X	X	X	X	X	X	X	X	X
Resistance to Permanent Deformation - Unconditioned Flow Number (FN): 3 samples	X	X	X	X	X	X				
Resistance to Thermal Cracking - Unconditioned TSRST: 3 samples	X	X	X	X						

Table 3 Aggregate Gradation by Percent Passing and Bin Percentages Used.

Sieve size (mm)	3/4"	1/2"	3/8"	Rock Dust	Wade Sand	Hydrated Lime	RAP	Combined Grading	Job Mix Formula	Design Specification
25.0 mm (1 in)	100	100	100	100	100	100	100	100	100 - 100	100 - 100
19.0 mm (3/4 in)	100	100	100	100	100	100	100	100	93 - 100	90 - 100
12.5 mm (1/2 in)	45	100	100	100	100	100	100	90		
9.5 mm (3/8 in)	11	47	99	100	100	100	96	77	70 - 84	63 - 85
4.75 mm (No. 4)	2	1	23	95	99	100	72	49	45 - 56	45 - 65
2.36 mm (No. 8)	1	1	2	73	97	100	54	37		
2.00 mm (No. 10)	1	1	1	65	97	100	50	34	30 - 38	30 - 44
1.18 (No. 16)	1	1	1	45	93	100	41	28		
600 um (No. 30)	1	1	1	29	75	99	31	21		
425 um (No. 40)	1	1	1	24	53	99	26	17	13 - 21	12 - 22
300 um (No. 50)	1	1	1	20	30	99	22	13		
150 um (No. 100)	1	1	0	15	7	99	15	8		
75 um (No. 200)	0.8	0.4	0.4	11.4	1.6	86.4	10.7	5.5	3.6 - 7.6	3 - 8
Bin Percentages: 3/4" = 18.4, 1/2" = 10.5, 3/8" = 22%, Rock Dust = 20.7, Wade Sand = 11.9%, RAP = 15.0, Lime = 1.3										

Table 4 Mix Design Summary and Specifications.

Property	Bravo Ave	Specifications
Asphalt Binder Grade	PG64-28	--
Mixing Temperature Range, Viscosity Based (°C)	160-166	--
Compaction Temperature Range, Viscosity Based (°C)	150-155	--
Number of Compaction Blows	50	--
Hydrated Lime (%DWVA*)	1.5	--
RAP Content (%)	15.0	
RAP Binder Content (%TWM*)	4.25	--
Total Design Binder Content (% TWM*)	5.1	--
RAP Binder Replacement (% TWM*)	0.6	--
Design Air Voids (%)	4.0	4.0
Voids in Mineral Aggregates (%)	13.2	13 Min.
Voids Filled with Asphalt (%)	70.1	65-75
Marshal Stability (lbs)	3,386	1,800 Min.
Marshal Flow (0.01 inches)	14	8-20

*DWVA and TWM denotes “Dry Weight of Virgin Aggregate” and “Total Weight of Mix,” respectively

Table 5 Quality Assurance Testing Conducted by Wood Rogers on Bravo Avenue Field HMA and WMA Mixtures.

Project:	Bravo Avenue Rehabilitation																						
Project No.:	8312.005																						
Material:	Type 2 PG64-28NV RAP 50 Blow 4% Air Void																						
Supplier:	Granite Construction																						
Contractor:	Granite Construction																						
Station				16+60	34+10	40+12	62+33	15+00	33+00	50+50	14+00	26+11	14+50	27+50	46+15	62+23	48+50	12+85	28+85	36+85	42+85	52+85	66+85
Side				Right	Right	Right	Right	Left	Right	Left	Right	Right	Left	Left	Left	Left	Right	Right	Right	Right	Left	Left	Left
Lift				Bottom	Bottom	Bottom	Bottom	Bottom	Bottom	Top	Top	Top	Top	Top	Top	Top	Top	Top	Top	Top	Top	Top	Top
Lot				740	741	742	743	744	745	746	748	749	750	751	752	753	754	748	749	750	752	752	753
Type				HMA	WMA	WMA	WMA	WMA	WMA		HMA	WMA	WMA	WMA	WMA	WMA		HMA	WMA	WMA	WMA	WMA	WMA
Date Sampled				8/30	8/30	8/30	8/30	8/30	8/30	8/30	8/31	8/31	8/31	8/31	8/31	8/31	8/31	8/31	8/31	8/31	8/31	8/31	8/31
Avg. Core Thickness (in)				6.4	6.1	6.1	6.3	6.2	6.2	6.4	6.4	6.1	6.1	6	6.2	6.2	6.4	6.6	6.4	6.2	6.5	6	6.6
Avg. Lift Thickness (in)				2.88	2.63	2.58	2.87	2.82	2.87	2.92	3.15	3.18	3.08	3.15	3	2.83	2.9	2.95	2.85	2.85	3.2	3.1	2.95
Avg. Core Density (pcf)				144.3	143.8	144.9	144.5	144.6	143.3	144.3	146.4	146.5	144.6	143.9	145.8	145.2	145.8	143.4	145	145	143.8	142.1	142
Maximum Theoretical (pcf)				152.6	152.5	152.5	152.6	152.8	152.8	152.8	152.1	152.3	152.6	152.8	153	152.7	152.8	152.1	152.3	152.6	153	152.8	152.7
Avg. Theoretical Compaction (%)				95	94	95	95	95	94	94	96	96	95	94	95	95	96	94	95	95	94	93	93
Avg. Air Voids (%)				5.4	5.7	5	5.3	5.4	6.1	5.6	3.8	3.8	5.3	5.8	4.7	4.9	4.5	5.7	4.8	5	6	7	7
Marshall Density (pcf)				146.6	145	145.3	145.6	145	145.8	146.2	145.9	144	144.4	144.2	143.4	143.5	143.9	145.9	144	144.4	143.4	143.8	143.5
Avg. Marshall Compaction (%)				98	99	100	99	100	98	99	100	102	100	100	102	101	101	98	101	100	100	99	99
Asphalt Content and Gradation by Ignition Method (ASTM D 6307)																							
Sieve Size	% Passing																						
	IMF	SPEC.																					
1"	100	100	100	100	100	100	100	100	100	100	100	100	100	100	100	100	100	100	100	100	100	100	
3/4"	93-100	90-100	100	100	100	100	100	100	100	100	100	100	100	100	100	100	100	100	100	100	100	100	
1/2"	-	-	88	88	89	85	87	89	89	86	91	92	89	89	90	86	86	91	92	89	89	90	
3/8"	70-84	63-85	73	75	76	73	75	78	75	74	79	78	76	75	78	75	74	79	78	75	75	78	
#4	45-56	45-65	48	46	47	46	47	50	48	46	51	48	47	46	49	47	46	51	48	46	46	49	
#10	30-38	30-44	33	30	31	31	31	33	32	31	34	32	32	31	32	31	31	34	32	31	31	32	
#16	-	-	27	25	26	25	26	27	26	26	28	27	26	25	26	26	26	28	27	25	25	26	
#40	13-21	12-22	17	16	17	16	16	17	16	16	18	17	16	16	16	16	16	18	17	16	16	16	
#100	-	-	8	7	9	7	7	8	7	8	8	7	7	7	7	7	8	8	7	7	7	7	
#200	3-8	3-8	5.7	5.3	5.4	5	5.3	5.5	5.2	5.6	5.7	5.3	5.2	5	5.3	5.1	5.6	5.7	5.3	5	5	5.3	
% AC (TWM)	4.6		4.8	4.8	5	5	5	5.1	5.1	4.6	5	5	4.8	4.7	4.8	4.8	4.6	5	5	4.7	4.7	4.8	
Theor. Max. SP. Gravity (Rice):	-		2.452	2.45	2.451	2.451	2.455	2.451	2.455	2.444	2.447	2.452	2.454	2.457	2.454	2.457	2.444	2.447	2.452	2.457	2.457	2.454	
Marshall Compacted Test Data (Average of Three Specimens) (ASTM D 6926)																							
		SPEC.																					
Unit Weight, pcf:	-		146.6	145	145.3	145.6	145	145.8	146.2	145.9	144	144.4	144.2	143.4	143.5	143.9	145.9	144	144.4	143.4	143.4	143.5	
Stability, lbs.:	1800 min.		3290	2410	2560	2500	2300	2570	2755	3190	2810	2350	2590	2540	2600	2470	3190	2810	2350	2540	2540	2600	
Flow, 0.01 inch:	8-20		16	13	15	14	14	13	14	13	14	13	14	19	16	15	13	14	13	19	19	16	
Air Voids, %:	3-5		3.9	4.9	4.7	4.6	5.1	4.4	4.4	4.1	5.5*	5.4*	5.9*	6.2*	6*	5.8*	4.1	5.5	5.4	6.2	6.2	6	
In-Situ Test Data (Average of Three Cures) (ASTM D 2726-96)																							
Cure No.		SPEC.	1-3	4-6	7-9	10-12	13-15	16-18	1-3	1-3	4-6	7-9	10-12	13-15	16-18	1-3	1-3	4-6	7-9	10-12	13-15	16-18	
Thickness, in.:			3	6.4	6.1	6.1	6.3	6.2	6.4	6.4	6.1	6.1	6	6.2	6.2	6.4	6.6	6.4	6.2	6.5	6	6.6	
Unit Weight, pcf:			-	144.3	143.8	144.9	144.5	144.6	143.3	144.3	146.4	146.5	144.6	143.9	145.8	145.2	145.8	143.4	145	145	143.8	142.1	142
Relative Compaction																							
		SPEC.																					
Marshall, %:	96 min.		98	99	100	99	100	98	99	100	102	100	100	102	101	101	98	101	100	100	99	99	
Rice, %:	92-97		95	94	95	95	95	94	94	96	96	95	94	95	95	96	94	95	95	94	93	93	
Air Voids, %:	3-8		5.4	5.7	5	5.3	5.4	6.1	5.6	3.8	3.8	5.3	5.8	4.7	4.9	4.5	5.7	4.8	5	6	7	7	

* Out of Job Specification Tolerance

Table 6 Asphalt Binder Content of Field Mixtures from Plant Production.

Project	Mixture ID	Number of Samples	Asphalt Binder Content			JMF
			Average (%)	Standard Deviation	95% Confidence Interval	
Bravo Avenue	WMA_64-28	15	4.9	0.14	4.8-5.0	4.6-5.6
	HMA_64-28	3	4.7	0.12	4.5-4.8	

Table 7 Superpave PG Grades of Various Asphalt Binders.

	Binder	PG Grade
	Virgin	64-34
	RAP	82-16
(Extracted & Recovered)	FMLC_HMA_NoReheat	70-28
	FMLC_WMA_NoReheat	70-28
	FMLC_HMA_Reheat	70-16
	FMLC_WMA_Reheat	70-16
	LMLC_HMA_NoReheat	70-16
	LMLC_WMA_NoReheat	70-16
	LMLC_HMAatWMA_NoReheat	70-22

Table 8 Dynamic Modulus Values and Ratios of Field Mixtures at 10 Hz and 70°F.

Mix	$ E^* $, (ksi) at 70°F		
	0 F-T	1 F-T	6 F-T
HMA-No Reheat	428 --	388 (91%)	352 (82%)
HMA-Reheat	559 --	458 (82%)	460 (82%)
WMA-No Reheat	392 --	377 (96%)	339 (86%)
WMA-Reheat	443 --	393 (89%)	412 (93%)

Table 9 Dynamic Modulus Values and Ratios of Laboratory Mixtures at 10 Hz and 70°F.

Mix	$ E^* $, (ksi) at 70°F		
	0 F-T	1 F-T	6 F-T
HMA-No Reheat	564 --	451 (80%)	287 (51%)
HMA-Reheat	585 --	378 (65%)	327 (56%)
WMA-No Reheat	533 --	456 (86%)	325 (61%)
WMA-Reheat	615 --	395 (64%)	378 (61%)
HMA at WMA-No Reheat	530 --	448 (85%)	300 (57%)
HMA at WMA-Reheat	582 --	372 (64%)	275 (47%)

Table 10 Statistical Evaluation of Dynamic Modulus Results.

Comparison Type		P-Value	Significance
FMLC vs LMLC	Mix Type	0.287	Not Significant
	FMLC or LMLC	0.536	Not Significant
	Reheat/NoReheat	0.344	Not Significant
	F-T Cycling	0.000	Highly Significant
FMLC Reheat/NoReheat	Mix Type	0.000	Highly Significant
	Reheat/NoReheat	0.000	Highly Significant
	F-T Cycling	0.000	Highly Significant
LMLC Reheat/NoReheat	Mix Type	0.344	Not Significant
	Reheat/NoReheat	0.231	Not Significant
	F-T Cycling	0.000	Highly Significant
HMA vs WMA	Mix Type	0.538	Not Significant
	FMLC or LMLC	0.535	Not Significant
	Reheat/NoReheat	0.181	Not Significant
	F-T Cycling	0.003	Highly Significant

FIGURES



Figure 1 Double Barrel Green® WMA System.



Figure 2 Ultrafoam GX™ (Green Machine) WMA System.

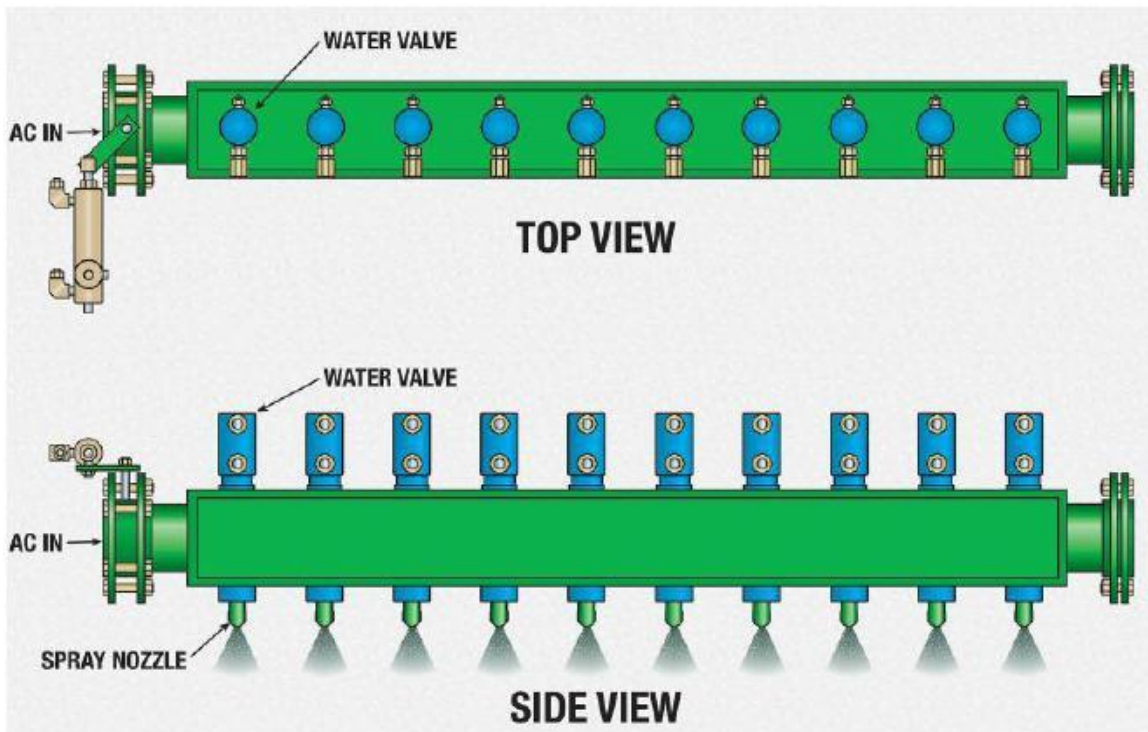


Figure 3 Double Barrel Green® Manifold.

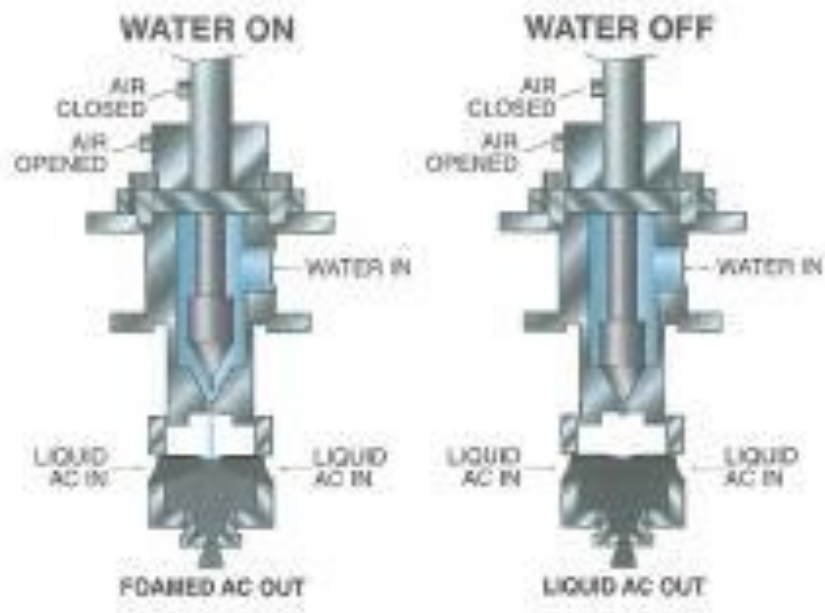


Figure 4 Double Barrel Green® Nozzle Schematic.



Figure 5 Maxam AQUABlack™ WMA System Unit Installed on a Drum Mix Plant.



Figure 6 AquaFoam Metering Skid.



Figure 7 AquaFoam Foaming Unit Installed in Asphalt Line.



Figure 8 Eco-Foam II Static Incline Vortex Mixer.



Figure 9 Terex® WMA System.

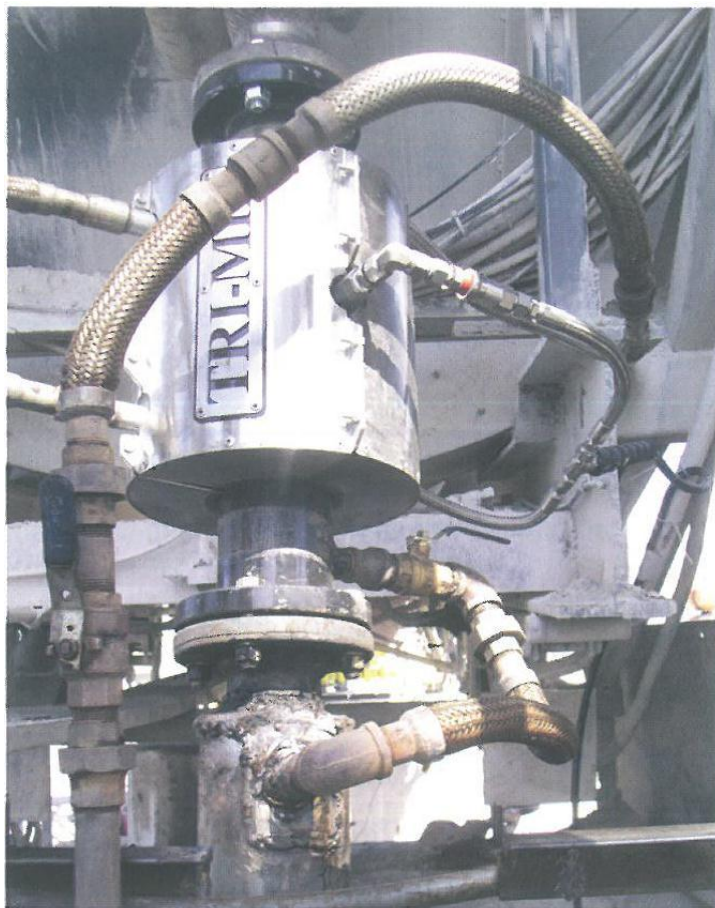


Figure 10 Tri-Mix Warm Mix Injection System.

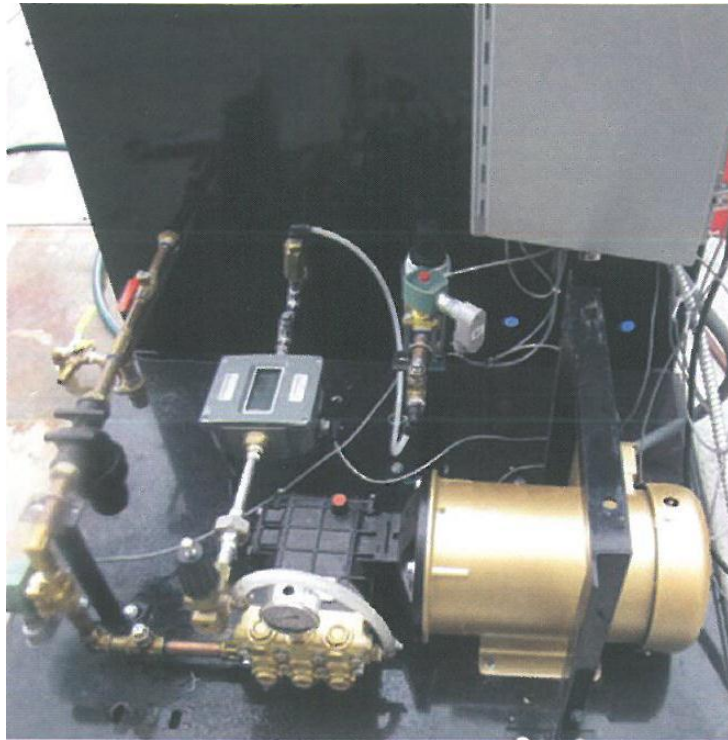


Figure 11 Pumping Skid for the Tri-Mix Warm Mix Injection System.



Figure 12 The Foamer and Disposable High Temperature Polymer Bag Manufactured by Pavement Technology, Inc.

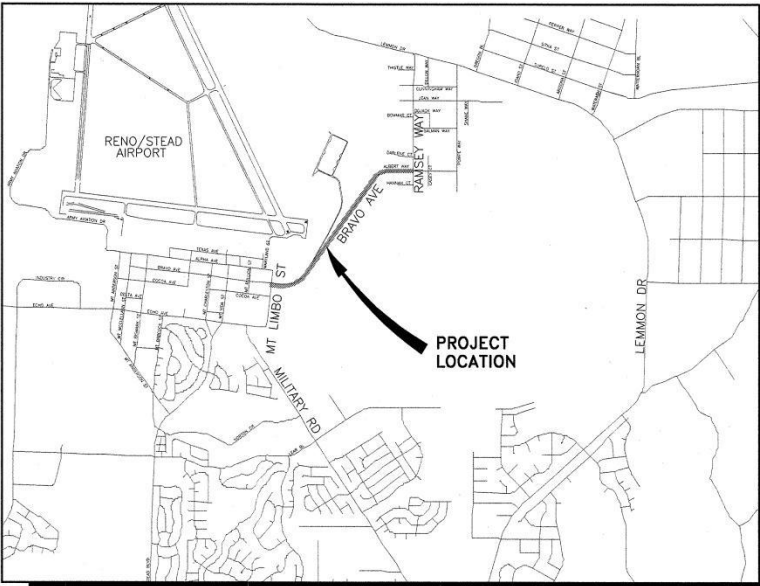


Figure 13 Location Map of Bravo Ave Field Project.

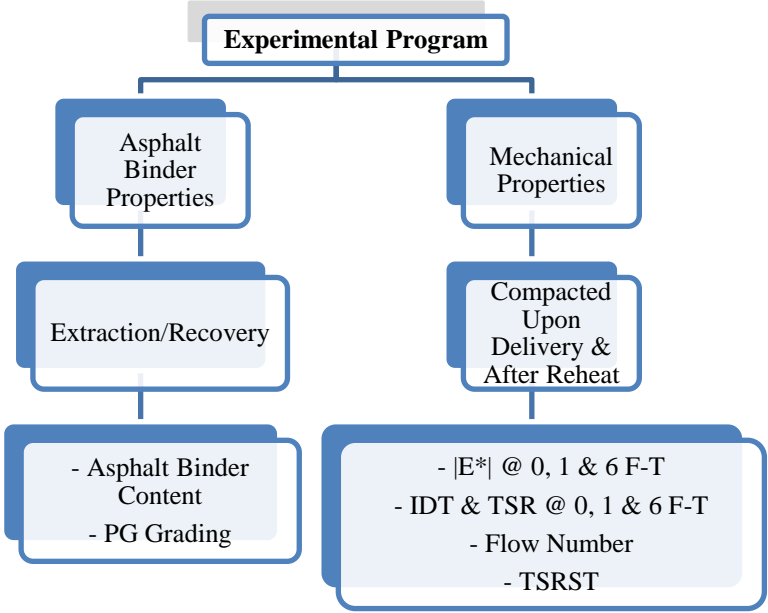


Figure 14 Study Experimental Program.

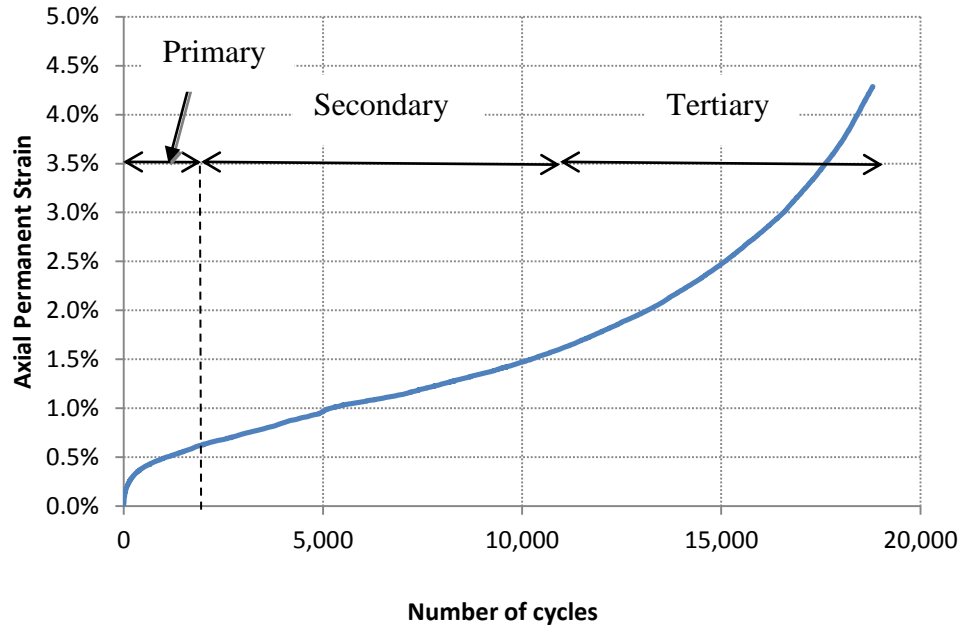


Figure 15 Cumulative Permanent Axial Strain with Respect to Number of Cycles.

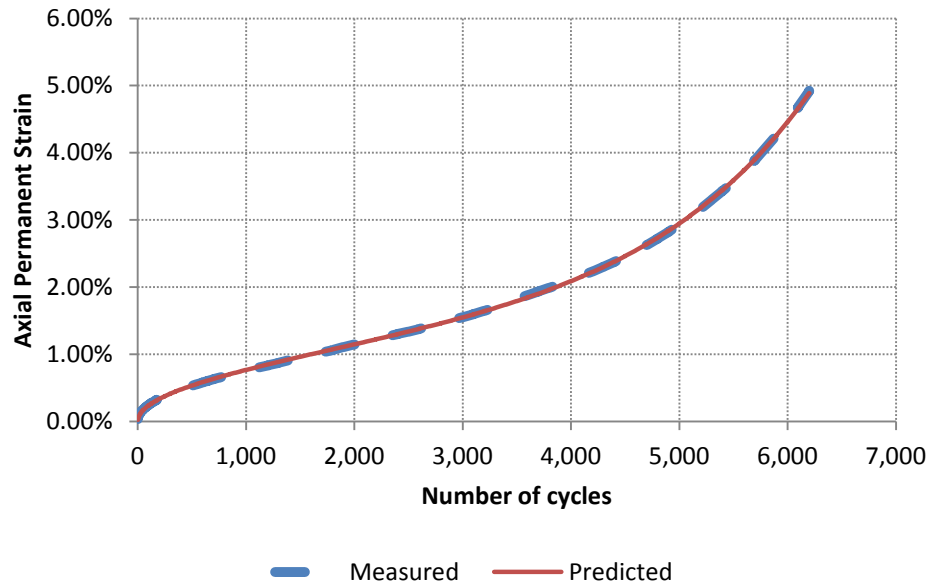


Figure 16 Typical Permanent Strain vs Loading Cycle Fitted with the Francken Model.

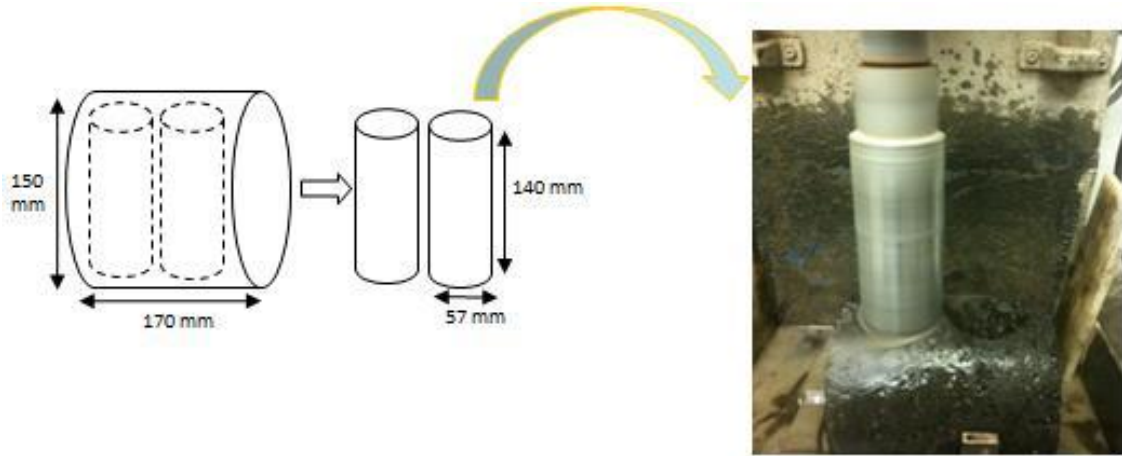


Figure 17 Coring of TSRST Samples.



Figure 18 Prepared TSRST Sample in Testing Chamber.

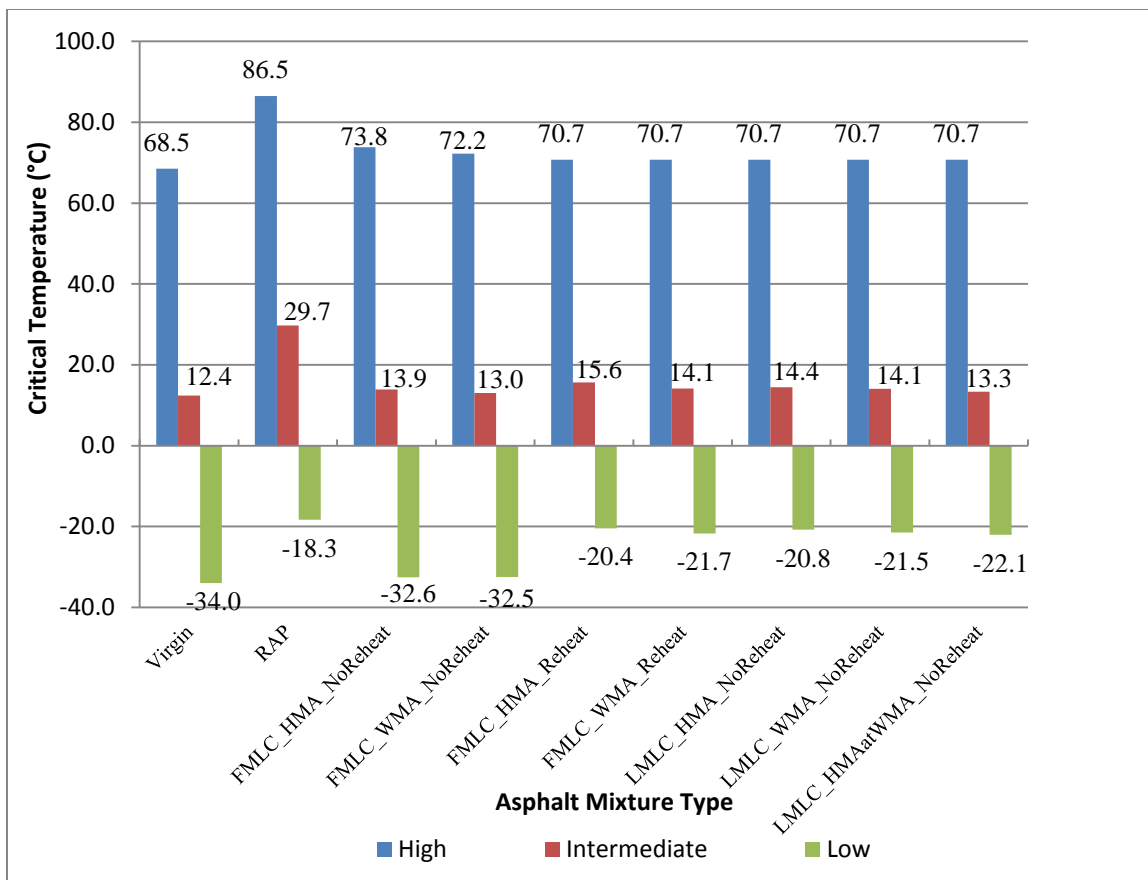


Figure 19 Superpave PG True Temperatures of Various Asphalt Mixtures.



Figure 20 |E*| of Field Mixtures at 70°F as a Function of F-T Cycles.

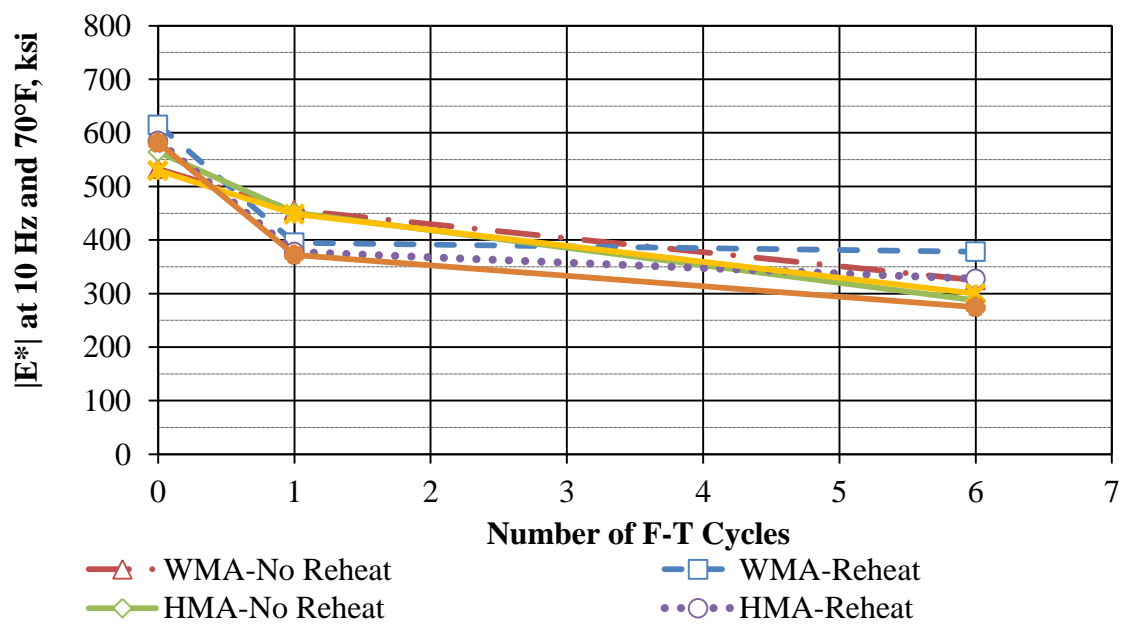


Figure 21 |E*| of Laboratory Mixtures at 70°F as a Function of F-T Cycles.

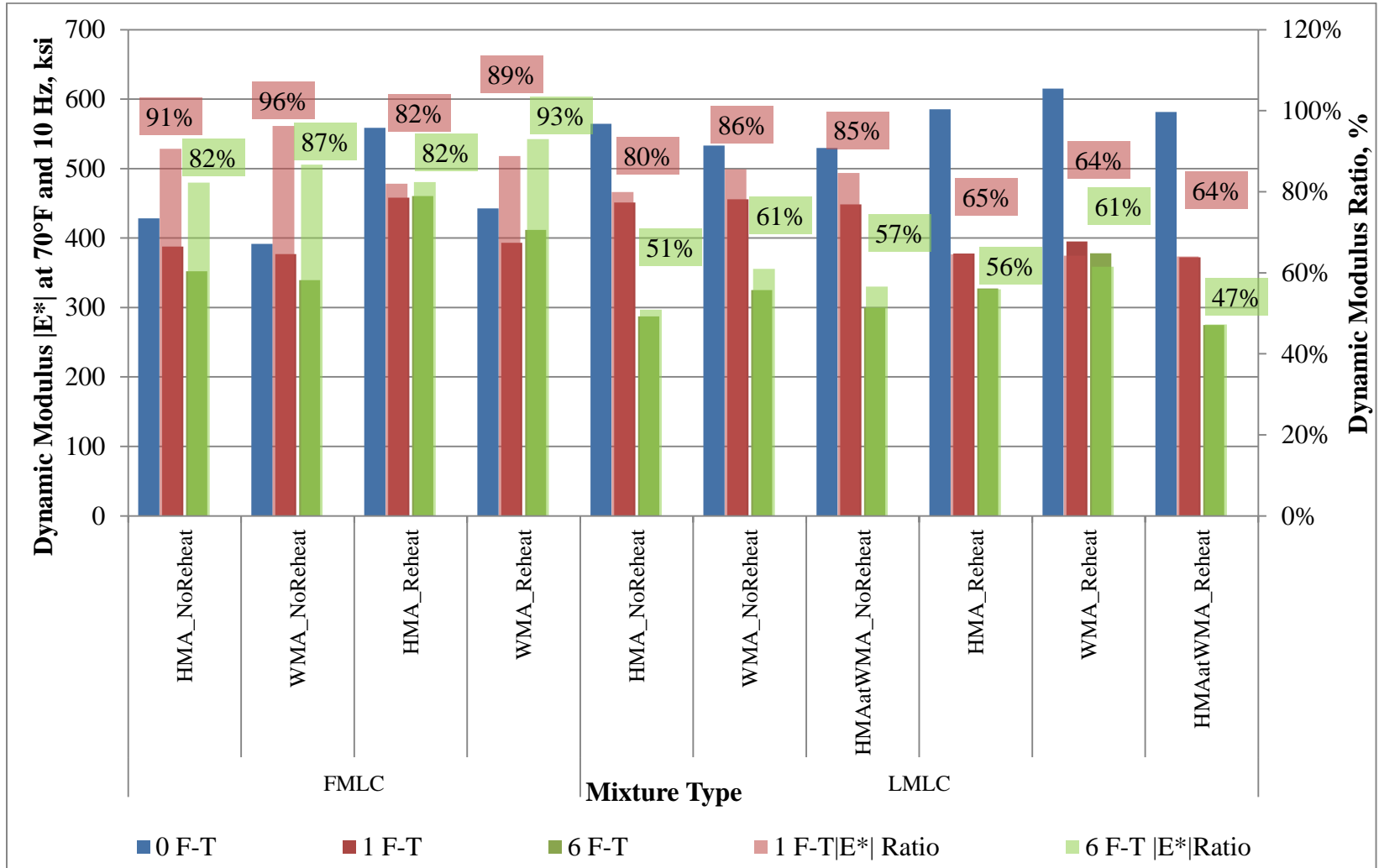


Figure 22 Dynamic Modulus and |E*| Ratios of All Field and Laboratory-Produced Mixtures.

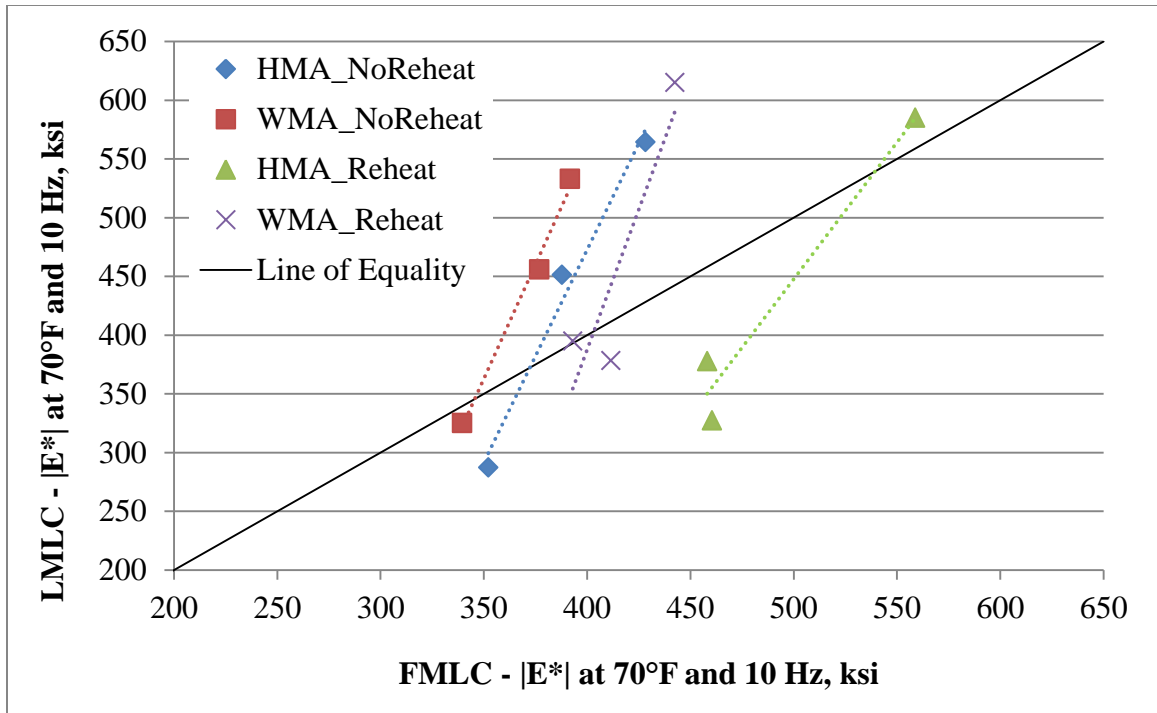


Figure 23 |E*| Comparison of Mixtures Produced in the Field and the Laboratory.

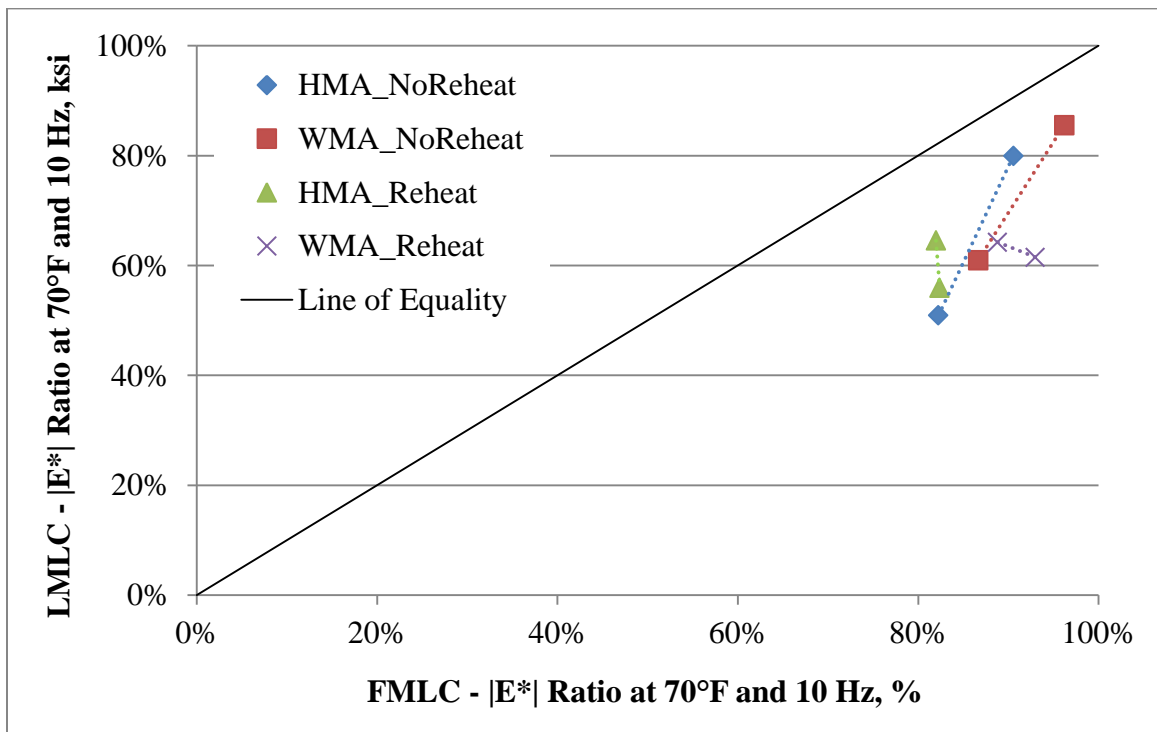


Figure 24 |E*| Ratio Comparison of Mixtures Produced in the Field and the Laboratory.

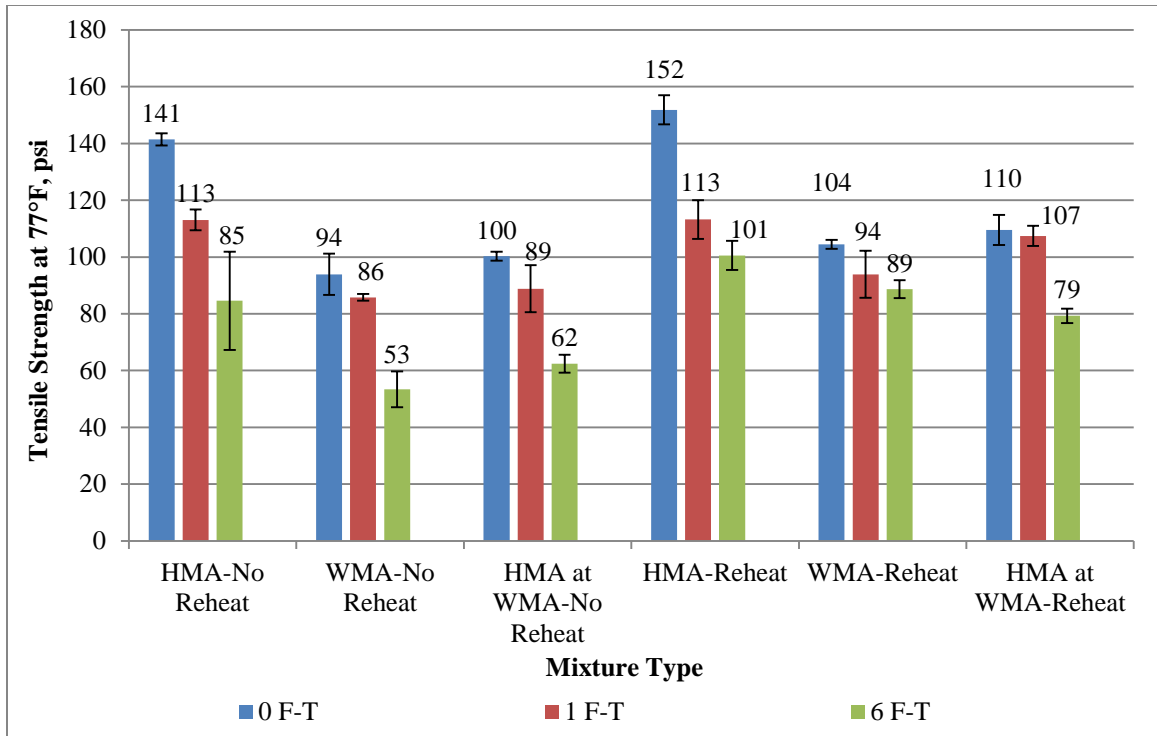


Figure 25 Tensile Strength of all Field-Produced Mixtures.

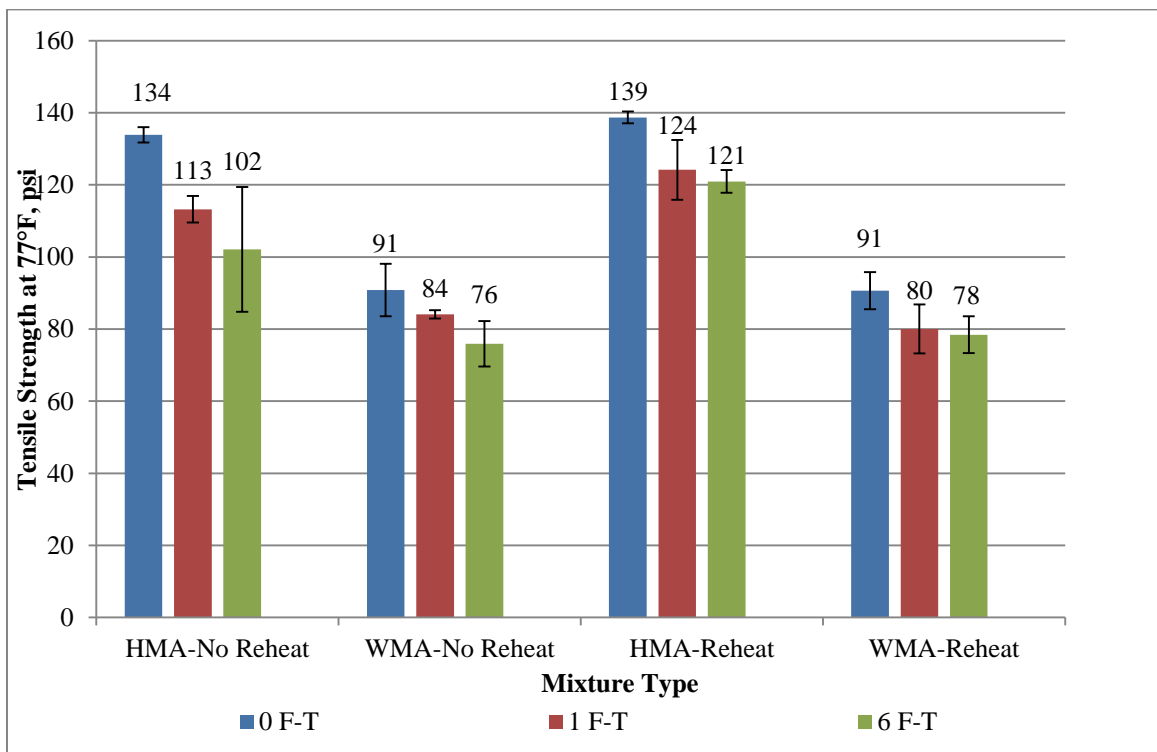


Figure 26 Tensile Strength of all Laboratory-Produced Mixtures.

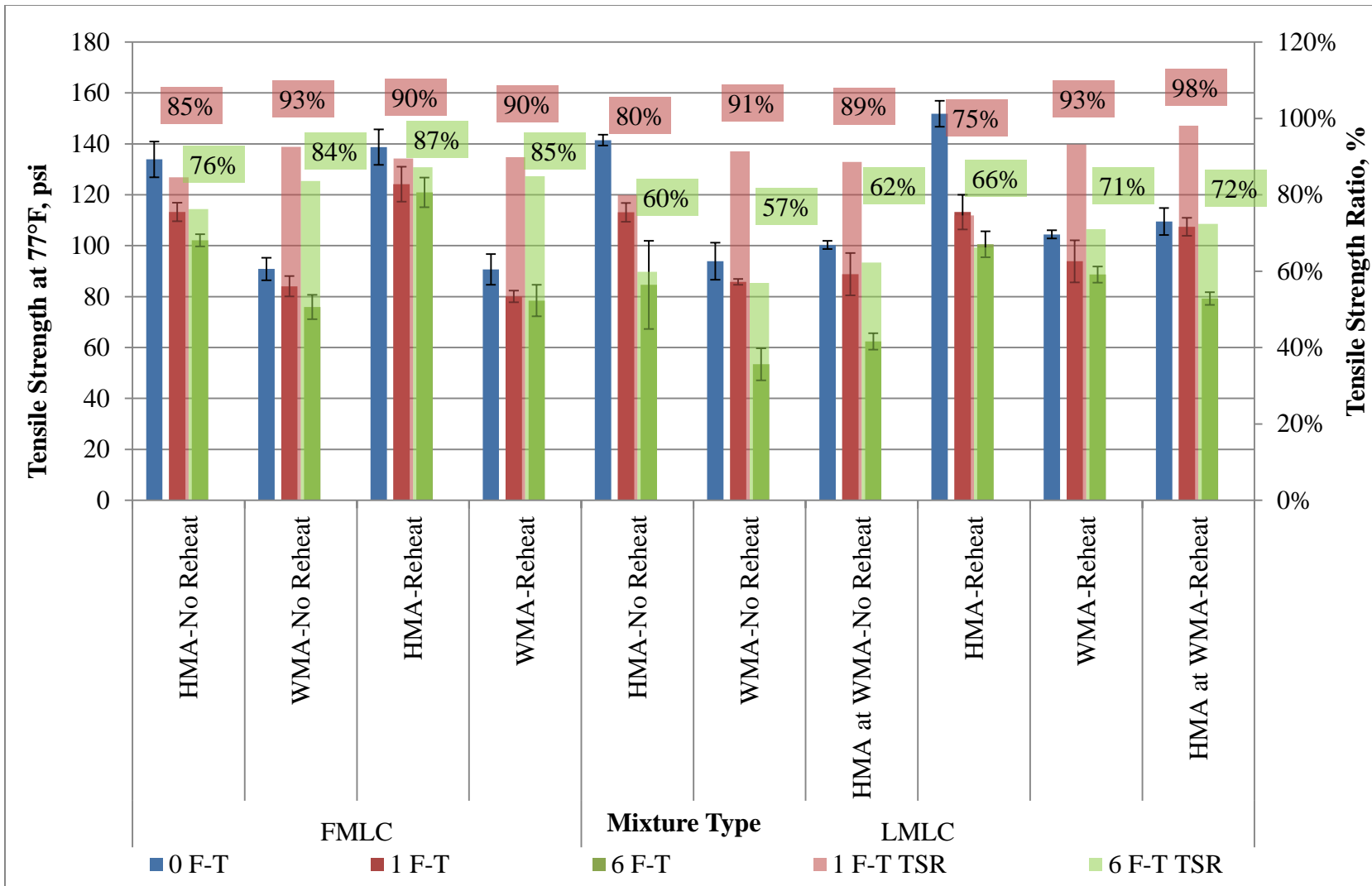


Figure 27 Tensile Strength and Tensile Strength Ratio of All Evaluated Field and Laboratory-Produced Mixtures.

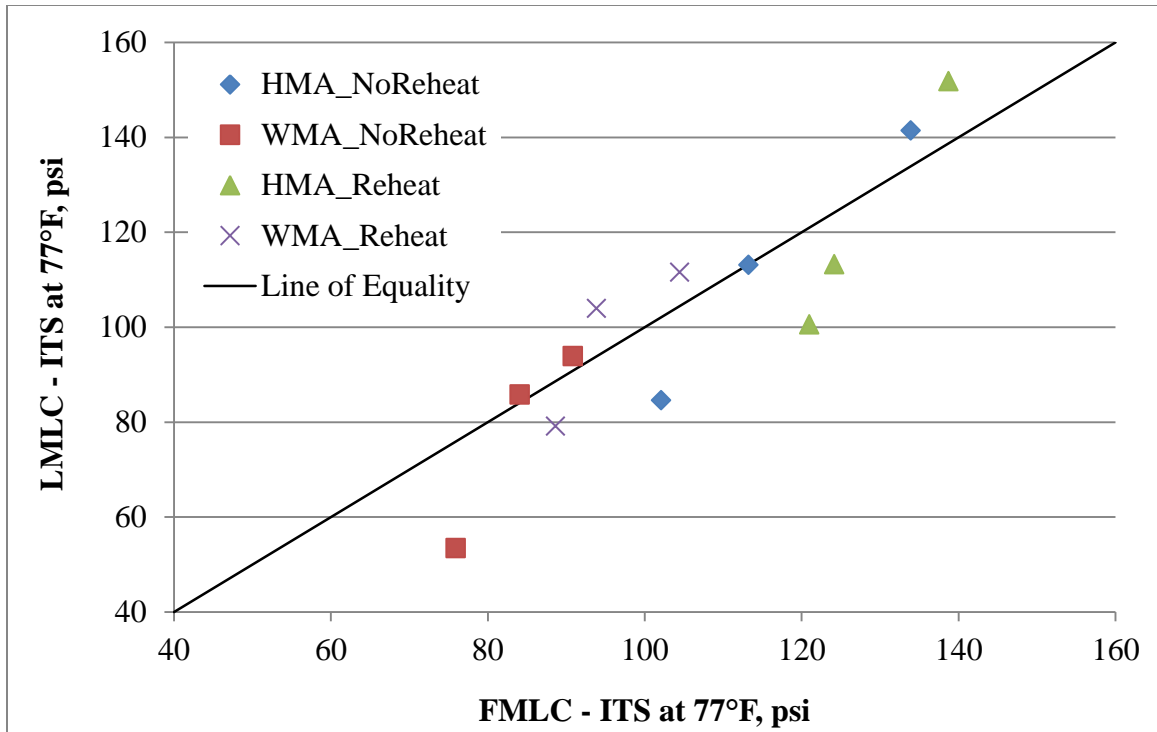


Figure 28 ITS Comparison of Mixtures Produced in the Field and the Laboratory.

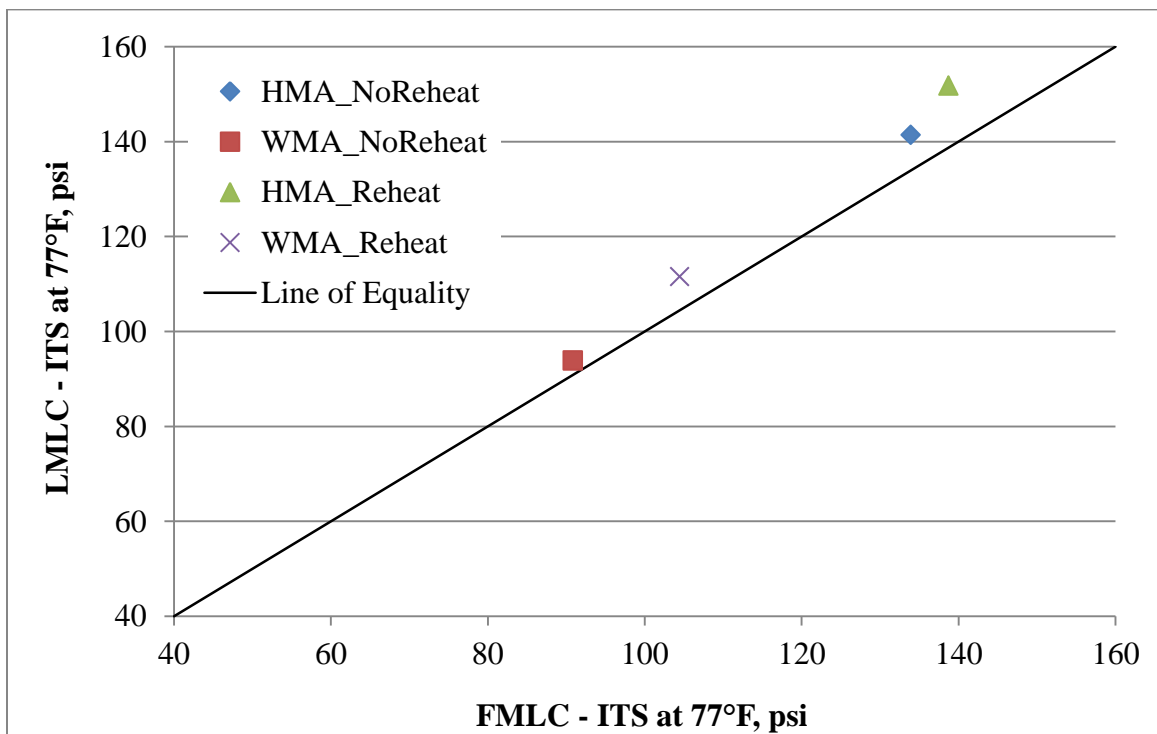


Figure 29 ITS Comparison of Mixtures Produced in the Field and the Laboratory (Dry).

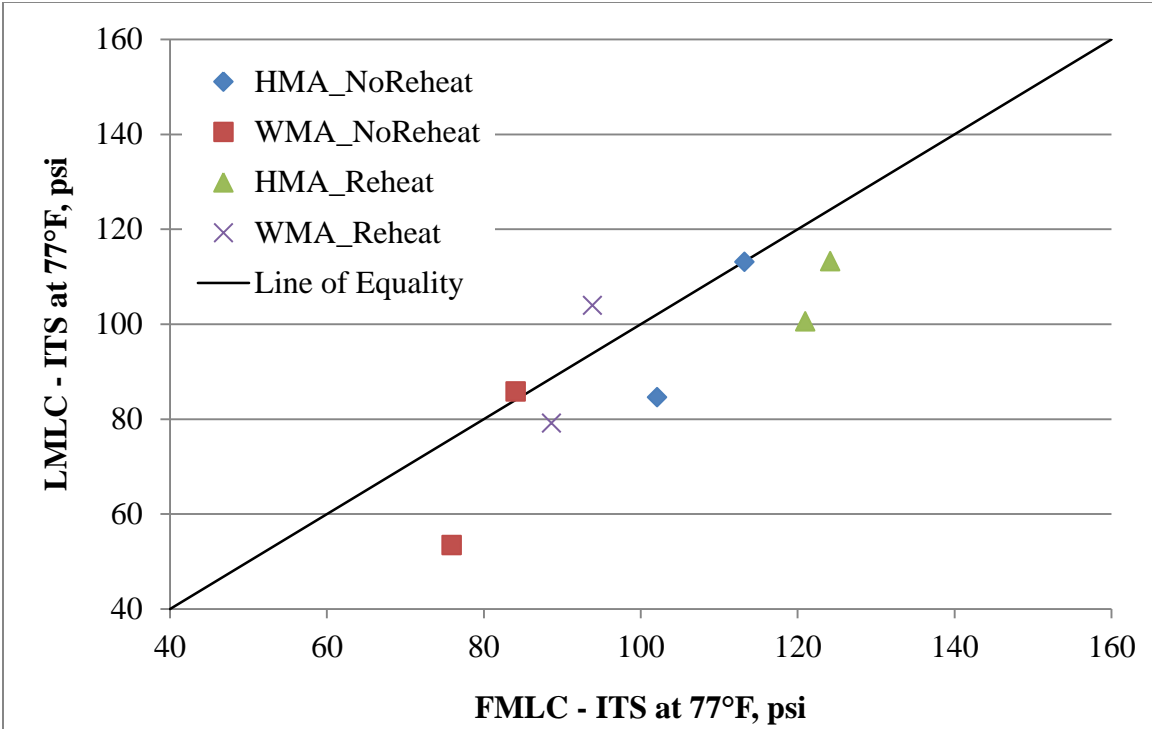


Figure 30 ITS Comparison of Mixtures Produced in the Field and the Laboratory (Wet).

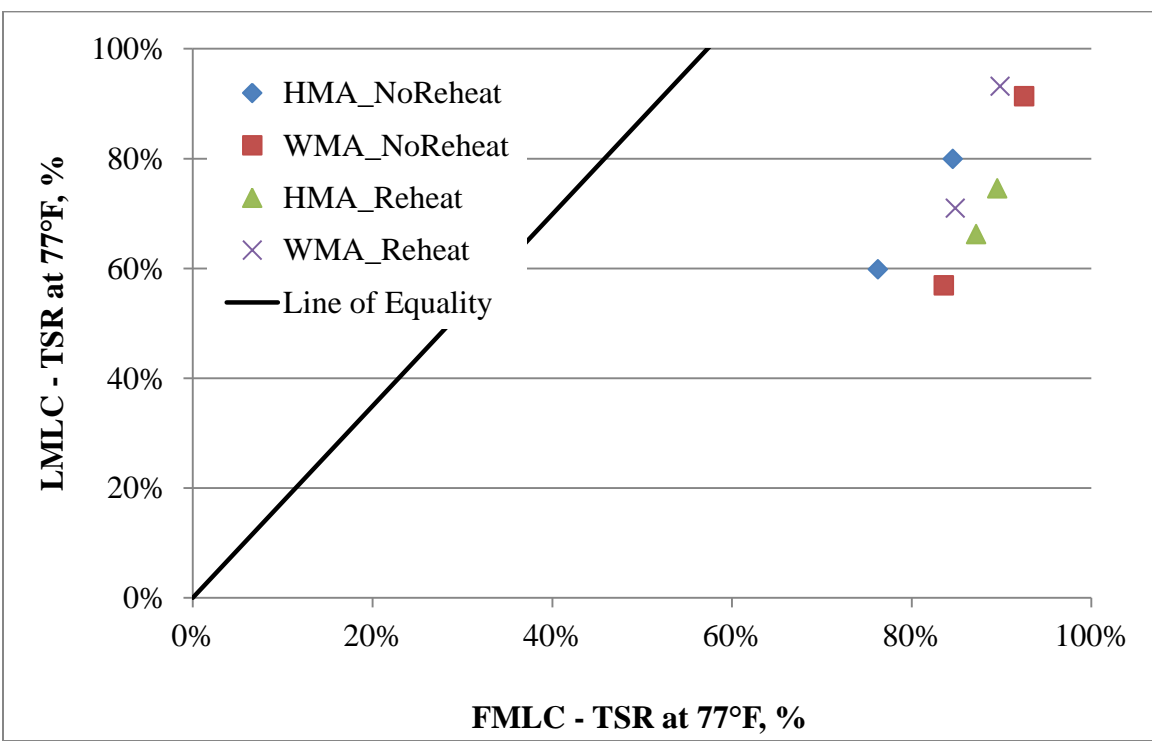


Figure 31 TSR Comparison of Mixtures Produced in the Field and the Laboratory.

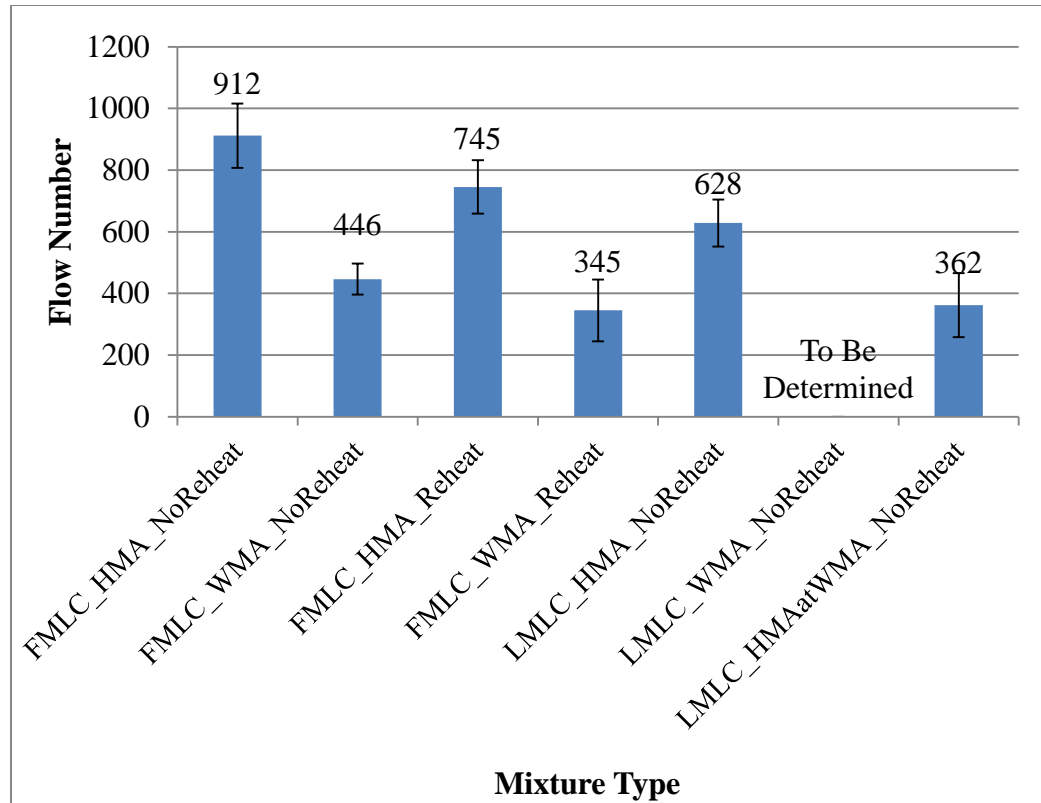


Figure 32 Flow Numbers at 58°C with 80 psi Deviator Stress and 30 psi Confining Stress. (Numbers represent mean values and whiskers represent mean \pm 95% confidence interval).

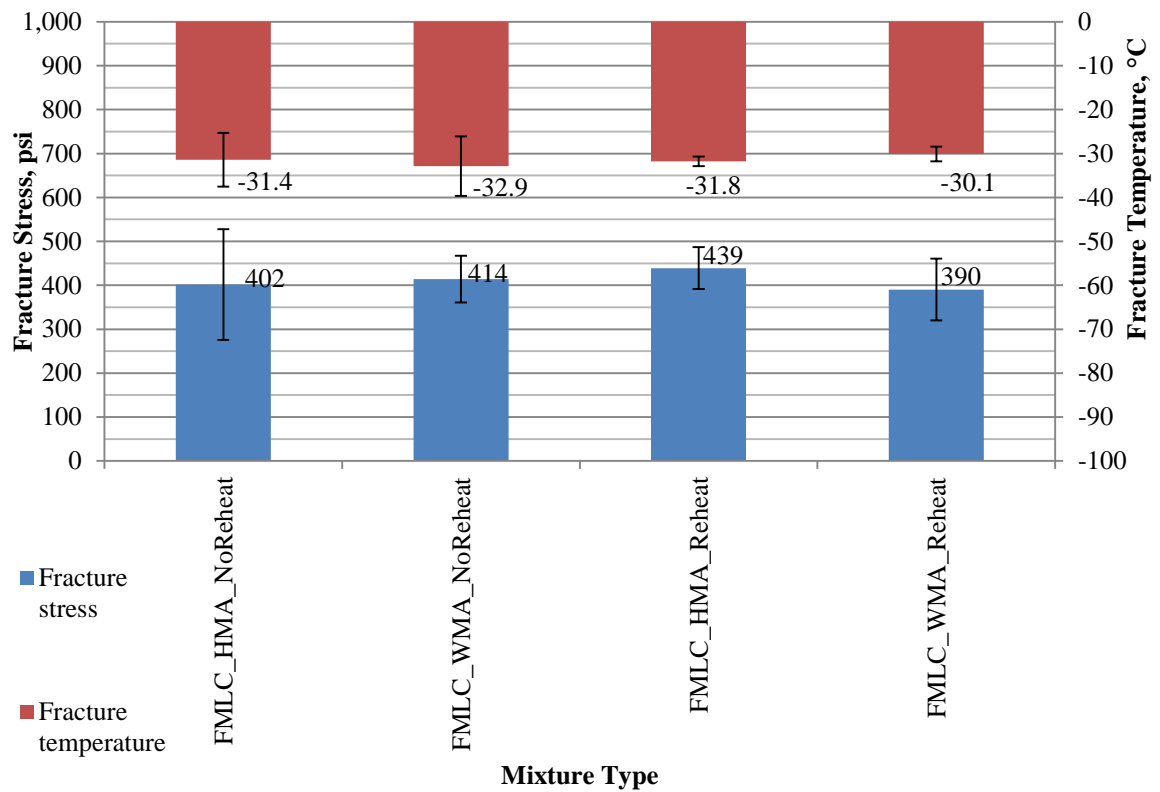


Figure 33 Fracture Stresses and Temperatures of FMLC Mixtures. (Numbers represent mean values and whiskers represent mean ± 95% confidence interval).



Figure 34 Photo for HMA and WMA Pavements on Bravo Avenue (May 18, 2011).

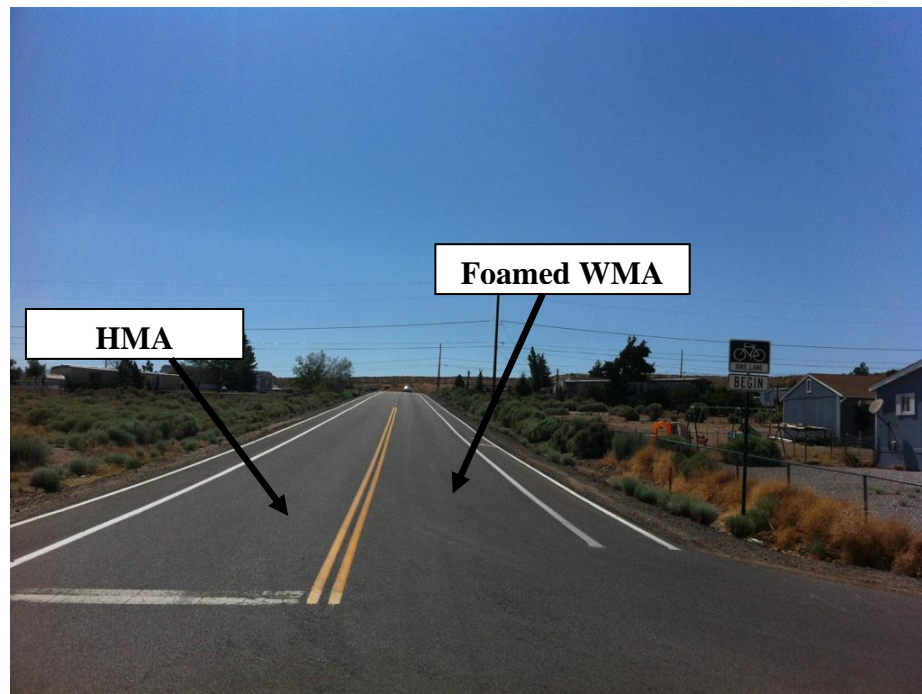


Figure 35 Photo for WMA and HMA Pavements on Bravo Avenue (July 17, 2012).



Figure 36 Maximum Rutting Depth of 1/16 Inches Measured (July 17, 2012).